Original Research

SPI1-Mediated Upregulation of the *CST1* Gene as an Independent Poor Prognostic Factor Accelerates Metastasis in Esophageal Squamous Cell Carcinoma (ESCC) by Interacting with MMP2

Fei-Fei Luo[1,†], Jing Wang[1,†], Zhan-Fei Zhang[1,2,†], Si-Ting Lin[1,3], Tie-Jun Huang[4], Bao-Qi Liu[1], Mei-Ling Fan[1], Li-Xia Peng[1], Shu-Tao Zheng[5], Chang-Fu Yang[6,*], Bi-Jun Huang[1,*]

[1]Department of Experimental Research, State Key Laboratory of Oncology in South China and Collaborative Innovation Center for Cancer Medicine, Sun Yat-sen University Cancer Center, 510060 Guangzhou, Guangdong, China

[2]Department of Cardiothoracic Surgery, Zhongshan People's Hospital, 529403 Zhongshan, Guangdong, China

[3]Department of Radiation Oncology, People's Hospital of Guangxi Zhuang Autonomous Region, 530021 Nanning, Guangxi, China

[4]Department of Nuclear Medicine, The Second People's Hospital of Shenzhen, 518035 Shenzhen, Guangdong, China

[5]Department of Clinical Medical Research Institute, State Key Laboratory of Pathogenesis, Prevention and Treatment of High Incidence Diseases in Central Asian, The First Affiliated Hospital of Xinjiang Medical University, 830011 Urumqi, Xinjiang, China

[6]Department of Oncology, The People's Hospital of Gaozhou, 6664126 Gaozhou, Guangdong, China

*Correspondence: yangchfu2013@163.com (Chang-Fu Yang); huangbj@sysucc.org.cn (Bi-Jun Huang)

[†]These authors contributed equally.

Academic Editor: Ilaria Baglivo

Submitted: 11 January 2023   Revised: 9 March 2023   Accepted: 4 April 2023   Published: 24 September 2023

Abstract

Background: Esophageal squamous cell carcinoma (ESCC) is a highly lethal tumor type, but studies on the ESCC tumor microenvironment are limited. We found that cystatin SN (CST1) plays an important role in the ESCC tumor microenvironment. CST1 has been reported to act as an oncogene in multiple human cancers, but its clinical significance and underlying mechanism in ESCC remain elusive. **Methods**: We performed ESCC gene expression profiling with data from RNA-sequencing and public databases and found CST1 upregulation in ESCC. Then, we assessed CST1 expression in ESCC by RT–qPCR and Western blot analysis. In addition, immunohistochemistry (IHC) and enzyme-linked immunosorbent assay (ELISA) were used to estimate the expression of CST1 in ESCC tissue and serum. Moreover, further functional experiments were conducted to verify that the gain and loss of CST1 in ESCC cell lines significantly influenced the proliferation and metastasis of ESCC. Mass spectrometry, coimmunoprecipation, and gelatin zymography experiments were used to validate the interaction between CST1 and matrix metalloproteinase 2 (MMP2) and the mechanism of CST1 influence on metastasis in ESCC. **Results**: Here, we found that CST1 expression was significantly elevated in ESCC tissues and serum. Moreover, compared with patients with low CST1 expression, patients with high CST1 expression had a worse prognosis. Overall survival (OS) and disease-free survival (DFS) were significantly unfavorable in the high CST1 expression subgroup. Likewise, the CST1 level was significantly increased in ESCC serum compared with healthy control serum, indicating that CST1 may be a potential serum biomarker for diagnosis, with an area under the curve (AUC) = 0.9702 and $p < 0.0001$ by receiver operating curve (ROC) analysis. Furthermore, upregulated CST1 can promote the motility and metastatic capacity of ESCC *in vitro* and *in vivo* by influencing epithelial mesenchymal transition (EMT) and interacting with MMP2 in the tumor microenvironment (TME). **Conclusions**: Collectively, the results of this study indicated that high CST1 expression mediated by SPI1 in ESCC may serve as a potentially prognostic and diagnostic predictor and as an oncogene to promote motility and metastatic capacity of ESCC by influencing EMT and interacting with MMP2 in the TME.

Keywords: CST1; esophageal squamous cell carcinoma (ESCC); metastasis; prognostic biomarker; tumor microenvironment (TME); matrix metalloproteinase (MMP)

1. Introduction

Esophageal cancer (ESCA) is one of the deadliest malignant cancers worldwide [1]. ESCA ranks sixth in cancer-related deaths and is the eighth most common cancer worldwide [2]. There is a high incidence of ESCA in China, and the morbidity and mortality of ESCA in China account for more than 50% of all ESCA-related events worldwide. Moreover, more than 90% of ESCA cases in China are esophageal squamous cell carcinoma (ESCC) [3]. Due to the challenges in early diagnosis and the lack of effective targeted therapeutic drugs, the outcomes of ESCC patients are dismal, with an approximately 30% five-year overall survival rate [4]. Although some studies have explored the pathogenesis of ESCC, the molecular mechanisms are still unclear. Therefore, it is necessary to further explore the underline molecular mechanism of ESCC tumorigenesis and develop more corresponding therapeutic approaches.

Several studies have conclusively confirmed an essential role of the tumor microenvironment (TME) in ESCA progression and metastasis. It has been demonstrated that the ESCA TME, except for the extracellular matrix (ECM), is enriched in tumor-associated fibroblasts, immune cells, proinflammatory cytokines, chemokines, and growth factors, and their complex crosstalk with each other or their receptors influences the development and progression of ESCA [5,6].

Comprehensive insight is needed into the complex interconnected components of the TME via these secretory factors in the TME, which can offer an opportunity to identify novel targets with diagnostic, prognostic, and therapeutic potential. Cystatin SN (CST1), a secretory protein encoded by the *CST1* gene, is a member of the type 2 cystatin superfamily of cysteine proteinase inhibitors [7], which plays crucial roles in promoting tumor progression during tumor development [8], including cell proliferation, migration, invasion, metastasis and recurrence [8]. Type 2 cystatin are usually secretory peptide and presumed to function extracellularly as a member of the extracellular matrix, which could been detected in a variety of fluids and secretions, including the plasma, saliva and tears [9]. The *CST1* gene contains three exons, and its coding DNA sequence (CDS) region has 426 nt bases, encoding only one protein and no other alternative splicing variants. CST1, a secreted protein, contains 141 amino acids and a molecular weight of approximately 17 kDa, while CST1 was detected in the cytoplasm, nucleus and extracellular matrix, so we speculate that CST1 may play different roles in different regions of the cell.

A study reported upregulated cysteine proteases, such as cathepsins, resulted in colorectal cell death [10]. Cysteine proteases functioned in protein degradation in lysosomes and secretory granules may act as tumor suppressors in tumor progression [11]. Specifically, cysteine peptidases are involved in remodeling ECM during development and are likely involved in tissue penetration by migrating cancer cells [12]. CST1 proteins also specifically inhibit the proteolytic activity of cysteine proteases [13]. Previous studies have indicated that CST1 is involved in the tumorigenesis of multiple cancers, such as lung cancer [14], colorectal cancer [15–17], liver cancer [18,19], pancreatic cancer [20], gastric cancer [21] and breast cancer [22,23].

The current research on CST1 in ESCA seems to be contradictory. In contrast to our study, one study reported that as an independent predictor of 5-year survival, overexpression of CST1 was associated with better survival of patients with ESCC based on immunohistochemistry (IHC) [24]; however, since this research was limited to the IHC method and clinical parameter analysis, the definitive role of CST1 in ESCC and its mechanisms remain ambiguous. Another study showed that high expression of CST1 in the ECM was associated with poor prognosis in ESCC. However, this study is only based on bioinformatics analysis,

and further experimental verification is needed [25]. Therefore, the role of CST1 in ESCC remains unclear.

In addition, we mainly investigated the role of CST1 as a secreted protein in the TME by interacting with the matrix metalloproteinase (MMP) family member MMP2. The MMP family belongs to the family of Ca^{2+} and Zn^{2+}-dependent proteolytic enzymes. Depending on their substrate specificity, MMPs are broadly divided into collagenases, strome lysins and gelatinases. The latter group, comprising gelatinase A (72 kDa type IV collagenase, MMP2) and gelatinase B (92 kDa type IV collagenase, MMP9), degrades denatured collagens (gelatin), native type IV and V collagens and elastin. It has been previously shown that MMPs function as potential ESCA diagnosis and/or prognosis biomarkers, including MMP1, MMP2, MMP3, MMP7, and MMP9, among which MMP2 and MMP9 are the most strongly involved in ESCA carcinogenesis and metastasis [26–29].

The results of this study revealed a pivotal role for CST1 in ESCC metastasis and tumorigenesis, which demonstrated that CST1 may be a potential prognostic biomarker and therapeutic target in ESCC. In addition, since CST1 is a secreted protein, high concentrations of CST1 can be detected in the blood of ESCC patients rather than normal people, so it can also be used as a potentially noninvasive early diagnostic method for ESCC patients.

2. Materials and Methods

2.1 Clinical Sample Collection

In total, 220 pathologically confirmed ESCC formalin-fixed, paraffin-embedded tissues and 19 matched tumor-adjacent samples were obtained from the Department of Pathology at the Sun Yat-Sen University Cancer Center (SYSUCC). Another 24 pairs of fresh primary ESCC tissues and corresponding normal tissues were collected from the Department of Thoracic Surgery at the First Affiliated Hospital of Sun Yat-Sen University (FAH-SYSU). Fifteen normal blood samples and 87 ESCC blood samples were collected from Gaozhou People's Hospital in Guangdong Province. All patients were untreated and had no history of other tumors. Written informed consent was obtained from all participants, and the research was approved by the Medical Ethical Committee of the SYSUCC.

2.2 Cell Lines and Cell Culture

The eight human ESCC cell lines (EC18, KYSE30/K30, Ec109, KYSE150/K150, KYSE180/K180, KYSE410/K410, KYSE510/K510, KYSE520/K520) and one immortalized normal esophageal cell line (NE1) used in the present study were kindly gifted by Professor Guan (Department of Clinical Oncology, University of Hong Kong). All cell lines were authenticated using the short tandem repeat (STR) technique. Additionally, mycoplasma testing was conducted on the cell lines, and the result is negative. Cells culture was by medium mixed with 10%

fetal bovine serum and a 1% penicillin–streptomycin in DMEM (Gibco, Carlsbad, CA, USA) at 37 °C under 5% CO_2.

2.3 Immunohistochemistry (IHC)

Immunohistochemical assays were carried out according to a protocol described by other researchers [30]. A CST1 antibody (diluted 1:200; Proteintech, #16025-1-AP, Chicago, USA) was used to stain for CST1. When staining was completed, two pathologists reviewed and scored the sections independently, and discrepancies in scoring were resolved by consensus. The mean score was used as a cut-off value to divide the samples into high and low CST1 expression groups. The expression level of CST1 in ESCC tissues was scored as the proportion of the area with positive staining (1 for 0–25%; 2 for 25–50%; 3 for 50–75%; 4 for 75–100%;) multiplied by the staining intensity (0 for negative; 1 for weak; 2 for moderate; 3 for intense).

2.4 RNA Extraction and Real-Time (RT)-Quantitative PCR (qPCR)

Total RNA was extracted from cells by using TRIzol reagent (Invitrogen, Carlsbad, CA, USA) following the manufacturer's instructions. The PrimeScript RT Master Mix Kit (Takara Bio, Kusatsu, Japan) was used for reverse transcription. RT–qPCR was carried out using a SYBR Green Master Mix Kit (YEASEN, Shanghai, China) according to the manufacturer's instructions, followed by a Roche 96/384-well Real-Time PCR system (Roche Applied Science, Indianapolis, IN, USA). GAPDH was used as an internal control. The primers used are listed in Table 1.

Table 1. Primers used in this study and their sequences.

Primer name	Sequence (5′-3′)
CST1 Forward:	TGTGCCTTCCATGAACAGCCAG
CST1 Reverse:	CTGGCACAGATCCCTAGGATTC
GAPDH Forward:	GTCTCCTCTGACTTCAACAGCG
GAPDH Reverse:	ACCACCCTGTTGCTGTAGCCAA
MMP-1 Forward:	ATGAAGCAGCCCAGATGTGGAG
MMP-1 Reverse:	TGGTCCACATCTGCTCTTGGCA
MMP-2 Forward:	AGCGAGTGGATGCCGCCTTTAA
MMP-2 Reverse:	CATTCCAGGCATCTGCGATGAG
MMP-3 Forward:	CACTCACAGACCTGACTCGGTT
MMP-3 Reverse:	AAGCAGGATCACAGTTGGCTGG
MMP-9 Forward:	GCCACTACTGTGCCTTTGAGTC
MMP-9 Reverse:	CCCTCAGAGAATCGCCAGTACT
MMP-10 Forward:	TCCAGGCTGTATGAAGGAGAGG
MMP-10 Reverse:	GGTAGGCATGAGCCAAACTGTG
MMP-13 Forward:	CCTTGATGCCATTACCAGTCTCC
MMP-13 Reverse:	AAACAGCTCCGCATCAACCTGC
HPRT Forward:	TTCCTTGGTCAGGCAGTATAATCC
HPRT Reverse:	AGTCTGGCTTATATCCAACACTTCG
ACTB Forward:	CAATGAGCTGCGTGTGGC
ACTB Reverse:	CGTACATGGCTGGGGTGTT

2.5 Preparation of Conditioned Medium (CM)

Cells (1×10^6) were plated in 100-mm dishes. After 12 h under normal culture conditions, the cells were starved for 48 h. Next, the conditioned medium was collected and centrifuged at 3000 rpm for 5 min, and the supernatant was concentrated in 250-μL Amicon Ultracentrifuge filters (MWCO = 10 kDa; Merck Millipore, Billerica, MA, USA). CST1 was detected by immunoblotting and other assays.

2.6 Migration Invasion and Wound Healing Assay

For this assay, 3×10^4 (migration) or 5×10^4 (invasion) stably transfected cells were seeded in triplicate on the top of a chamber equipped with 8-μm microporous filters with (invasion) or without (migration) a matrix coating. After incubation for 12 h (migration) or 24 h (invasion), the cells were harvested. The number of migrated or invaded cells in five random optical fields from triplicate filters was averaged. For the wound healing assay, 3×10^5 cells were plated in 6-well plates. Twenty-four hours later, wounds were made using a sterile 100-μL pipette tip. Debris was removed, and fresh medium was added. Images were captured at different times (0, 24, and 48 h). Additionally, we conducted another migration assay. Cultured K30-overexpressing and empty vector control cells were treated with isotype (diluted 1:50; Southern Biotech; Cat. No. 0107-01, Birmingham, USA) and CST1-neutralizing antibodies (diluted 1:50; Proteintech, #16025-1-AP, USA) for 12 h.

2.7 Western Blot Analysis

Western blot experiments were performed according to a protocol described by other researchers [31]. The antibodies used were as follows: CST1 rabbit monoclonal antibody (diluted 1:500; Proteintech, #16025-1-AP, Chicago, USA); GAPDH antibody (diluted 1:1000; Proteintech, #10494-1-AP, USA); MMP1 (Cell Signaling Technology, #54376, Danvers, MA, USA), MMP2 (Cell Signaling Technology, #40994, USA), MMP3 (Cell Signaling Technology, #14351, USA) and MMP10 antibodies (diluted 1:1000; Abcam, #ab261733, Cambridge, MA, USA); and E-cadherin (Proteintech, #20874-1-AP), Desmoplakin, N-cadherin (Proteintech, #22018-1-AP), Vimentin (Proteintech, #10366-1-AP), and Slug (diluted 1:1000; Proteintech, #12129-1-AP, USA), GAPDH was used as an internal reference. Enhanced chemiluminescence reagents were used to visualize the proteins.

2.8 Enzyme-Linked Immunosorbent Assay (ELISA)

An ELISA kit (Cloud-Clone Corporation, product No. SEJ330Hu 96 Tests) for CST1 and the serum sample dilution ratio used were performed according to the manufacturer's instructions. Specifically, a sandwich enzyme immunoassay for *in vitro* quantitative measurement of the CST1 protein concentration in human serum, human

plasma and cell culture supernatants was used. All the reactions were repeated three times. To make the calculation easier, we plotted the optical density (OD) value of the standard (X axis) against the known concentration of the standard (Y axis), to draw a standard curve. Then bring the detected OD value of the sample into the standard curve to obtain the specific concentration of the sample.

2.9 MTS and Colony Formation Assays

The MTS assay was used to assess cancer cell viability and growth. Cells (1000 in 200 µL of medium) were seeded into a 96-well plate (Jet Biofil; # TCP011096, Guangzhou, China) and cultured under normal conditions for 24 h. Thereafter, we diluted the Cell Titer 96 Aqueous One Solution Cell Proliferation Assay reagent (Promega; # G3581; Madison, WI, USA) at 1:100 with medium, added the diluted reagent to the cells and incubated the cells for 3 h. Cell growth curves were plotted using GraphPad software GraphPad Prism 7.0 (GraphPad Software Inc., San Diego, USA).

The cells were plated in 6-well plates (7.5×10^2/well) and cultured for 12 h to allow the cells to attach and cultured for 10 days until the colonies reached >50 cells. Next, the cells were harvested and fixed with methanol for 30 min and then stained with crystal violet for 1 h. Three different experiments were performed.

2.10 Dual Luciferase Assay

For the reporter assay, the cells were transiently transfected with the CST1 luciferase reporter plasmid (0.1 µg/well; Genecopoeia; HPRM18606-PG04, Rockville, MD, USA) and SPI1 expression plasmid (0.1 µg/well; Genecopoeia; EX-Z4319-Lv105) or empty vector (EV) in 96-well plates. Secreted Alkaline Phosphatase (SEAP) as an internal control (0.01 µg/well; Genecopoeia; pEZX-PA01). Forty-eight hours later, the luciferase assay was performed using the Secrete-Pair^{TM} Dual Luminescence Assay Kit (Genecopoeia, #LF031, USA) according to the manufacturer's protocol.

2.11 Construction of Lentiviral-Mediated Gaining or Loss of Function Stable Cell Line

Lentiviruses vector plasmids from the GeneCopoeia company (plasmids EX-A3184-Lv105 and EX-NEG-Lv105) were used to create stably expressing *CST1* or the vector cell lines, as well as stably knock down shRNA plasmids (HSH003349-21-LVRU6P, HSH003349-22-LVRU6P, HSH003349-23-LVRU6P, HSH003349-24-LVRU6P and CSHCTR001-LVRU6P) were used to construct stable expression cell lines. The targets of CST1 shRNA sequences we used were HSH003349-22-LVRU6P (KD22) 5′-GGTACTAAGAGCCAGGCAACA-3′ and HSH003349-24-LVRU6P (KD24) 5′-CAGAAGAAACAGTTGTGCTCT-3′. Overexpressing or knockdown lentiviruses vector plasmids were transfected into 293T cells by using Lipofectamine 3000 (Invitrogen,

#L3000150, Carlsbad, CA, USA) as a transfection reagent to produce the lentivirus according to the procedure of Lenti-Pac™ Lentiviral Packaging Systems (GeneCopoeia, #LT001, Rockville, MD, USA). Lentiviruses in 293T cell supernatant were harvested 72 h after transfection and filter through a 0.45-micron filter and freeze in an –80 degree refrigerator. Cells cultured with lentivirus and DMEM Medium (1:1) coupled with 2 µg/mL puromycin (sigma, #58-58-2, St. Louis, Missouri, USA) for stable cell lines selection within two weeks. Quantitative real-time PCR was used to detect the CST1 mRNA level; ELISA and immunoblotting were performed to determine the efficiency of CST1 protein level in overexpression or knockdown stable cells.

2.12 Coimmunoprecipitation Assay and Mass Spectrometry

After culturing cells with DMEM without serum for 24 h, the conditioned medium (CM) was collected and concentrated tenfold using an ultrafiltration device (from 10 mL to 1 mL) and mixed with CST1 antibody (diluted 1:500; Proteintech, USA) or isotype control (Southern Biotech; Cat: 0103-01) overnight at 4 °C. The cells were then mixed with protein A/G beads for 4 h at 4 °C. Then, the beads were washed 5 times with PBS. Finally, the beads were boiled with $1\times$ loading buffer for 10 minutes, and immunoblotting was carried out to determine whether CST1 was precipitated with MMP2 from the conditioned medium. The samples immunoprecipitated with CST1 and IgG antibodies were further subjected to mass spectrometry analysis by Shenzhen Weinafei Biotechnology Co., Ltd. (Shenzhen, China).

2.13 Gelatin Zymography Experiment

To obtain cell supernatants cultured in conditioned media, a total of 1×10^6 cells were seeded in 10×10-cm dishes with CM for two days, and total proteins were extracted from CM and separated via PAGE on 10% polyacrylamide gels containing 0.5% gelatin (Macklin, #G9136-10MG, Shanghai, China). The following steps were the same as those in a previous study [32]. The gels were incubated in substrate buffer for 24 h at 37 °C to enable MMP decompose substrate. Gels were stained with Coomassie Blue (BioFROXX, # 1078GR005, Guangzhou, China) for 2 h and washed until clear, and MMP decompose substrate was shown in the bright area.

2.14 Animal experiment

For the metastasis assay, female BALB/c nude mice aged 5 weeks old were purchased from Guangdong Laboratory Animal Center (Guangdong, China), and spontaneous lymph node (LN) metastasis experiments were conducted as previously reported [33]. Briefly, 2×10^5 cells stably expressing knockdown CST1 sequence with fluorescein tag in 20 µL mix of DMEM: matrigel (6:4) were subcutaneously injected into the footpad of each mouse to

generate a primary tumor. Take photos of fluorescent *in vivo* imaging once a week. After 4 weeks, the experiments were terminated, and the popliteal LNs were isolated and preserved in RNAlater solution (Invitrogen, USA). TRIzol was used for LN total RNA extraction, and real-time qPCR were then performed to assess metastasis using specific primers for hypoxanthine phosphoribosyltransferase 1 (human HPRT), which do not cross-react with the corresponding mouse gene [34] and ACTB (universal for humans and mice). The primer sequences are listed in Table 1.

For the tumorigenicity experiment, 2×10^6 cells suspended in 100 µL of DMEM containing 50% Matrigel (BD Biosciences) were subcutaneously inoculated into the subcutaneous area. The mice were monitored every three days for palpable tumor formation. Five weeks later, the mice were sacrificed and photographed, and the number of tumors was counted. All animal research protocols were approved by the at Sun Yat-sen University Cancer Center (SYSUCC) institutional Animal Care and Use Ethics Committee (IACUC), and the serial number of the protocol approved by IACUC was L102022021003K.

2.15 The Cancer Genome Atlas (TCGA) Data Analysis and Bioinformatics Analysis

The RNA-sequence data, microarray data and their corresponding clinical information were downloaded from TCGA and GEO databases (https://www.ncbi.nlm.nih.gov/gds), including 260 samples from the TCGA database (80 normal samples and 180 ESCA samples) and 238 samples from GEO datasets GSE53624 and GSE53625 (119 normal samples and 119 ESCA samples).

The ESCA samples were divided into CST1 high expression or CST1 low expression groups based on the cut off value with the median expression level. Kaplan–Meier survival analysis with the log-rank test was conducted to evaluate the difference in overall survival time between the two groups. The univariate and multivariate Cox regression were used to predict prognostic ability of CST1 expression, age, and grade based on samples from the TCGA and GEO databases. Hazard ratios (HRs) and 95% confidence intervals (CIs) were calculated accordingly. We constructed a nomogram based on CST1 expression, survival status and clinical characteristics to predict ESCC patient prognosis by R software. The time-dependent receiver operating characteristic (ROC) curve and area under the curve (AUC) were constructed to exam the prognostic predictive value of CST1 by the R software (R Foundation for Statistical Computing, Vienna, Austria), and the specific procedures are similar to we previously published article [35].

2.16 Statistics

Data were analyzed with SPSS (version 21.0) statistical software (IBM Inc., NY, USA). GraphPad Prism 7.0 (GraphPad Software Inc., San Diego, CA, USA) was used to visualize the data. For correlation analysis, the Pearson chi-square test was used to analyze the correlations between CST1 and clinical parameters. A two-tailed Mann–Whitney U test was used to compare differences between two groups of data. The Kaplan–Meier method with the log-rank test and the Cox multivariate proportional hazards regression model were applied for survival analysis, and $p < 0.05$ was considered statistically significant. Experimental data are presented as the mean $\pm$ s.d. of three independent experiments. $*p < 0.05$, $**p < 0.01$, $***p < 0.001$ by two-tailed Student's *t* test.

3. Results

3.1 CST1 Expression was Upregulated in ESCC Tissues

Our research focused on early-stage ESCC to identify new diagnostic or prognostic biomarkers; therefore, we tested the RNA profiles of three pairs of self-paired, early-diagnosis, untreated ESCC tissue and adjacent tumor tissue by RNA sequencing. Further analysis showed differentially expressed genes in a heatmap (Fig. 1A), where CST1 ranked first in overexpression among all the gene profiles. Then, we explored the expression of CST1 in ESCC in many databases. In the UALCAN database (http://ualcan.path.uab.edu/) [36], a differential expression heatmap showed that CST1 was one of the top 25 overexpressed genes in ESCC (**Supplementary Fig. 1A**), and the violin figure based on TCGA database indicated that CST1 expression was significantly higher in the 180 samples in ESCA group than the 80 samples in the normal group, $p < 0.001$ (Fig. 1B). Similar to TCGA, we downloaded two GEO (Gene Expression Omnibus) datasets (GSE53624 & GSE53625) and found that CST1 expression was significantly higher in the 119 ESCA samples than in the 119 normal group, $p < 0.001$ (**Supplementary Fig. 1F**).

In the Oncomine database (https://www.oncomine.com/) boxplots, the expression of CST1 in multiple cancers is shown in **Supplementary Fig. 1D**. Among those cancers, esophageal cancer showed the highest mean expression of CST1. In the ONCOMINE database, data from different investigators also showed that the expression level of CST1 in ESCC tissues was higher than that in normal tissues, and the difference was statistically significant, $p < 0.001$ (**Supplementary Fig. 1B,C,E**). Therefore, we explored the expression of CST1 in 12 pairs of ESCC self-paired untreated clinical tissue samples (Fig. 1C–E). In the 12 pairs of tumors with adjacent normal tissues, CST1 had significantly higher mRNA levels (Fig. 1C) and protein levels (Fig. 1D,E) in the tumor cells or tissues than in the normal counterparts. Then, we explored the CST1 expression level in pan-cancer and paired normal tissues in the TCGA database and found that CST1 was highly expressed in a variety of tumors, including ESCA (Fig. 1F).

3.2 CST1 was Associated with Relatively Poor Survival

Thus, we conducted IHC to detect the expression levels of CST1 in 220 formalin-fixed, paraffin-embedded
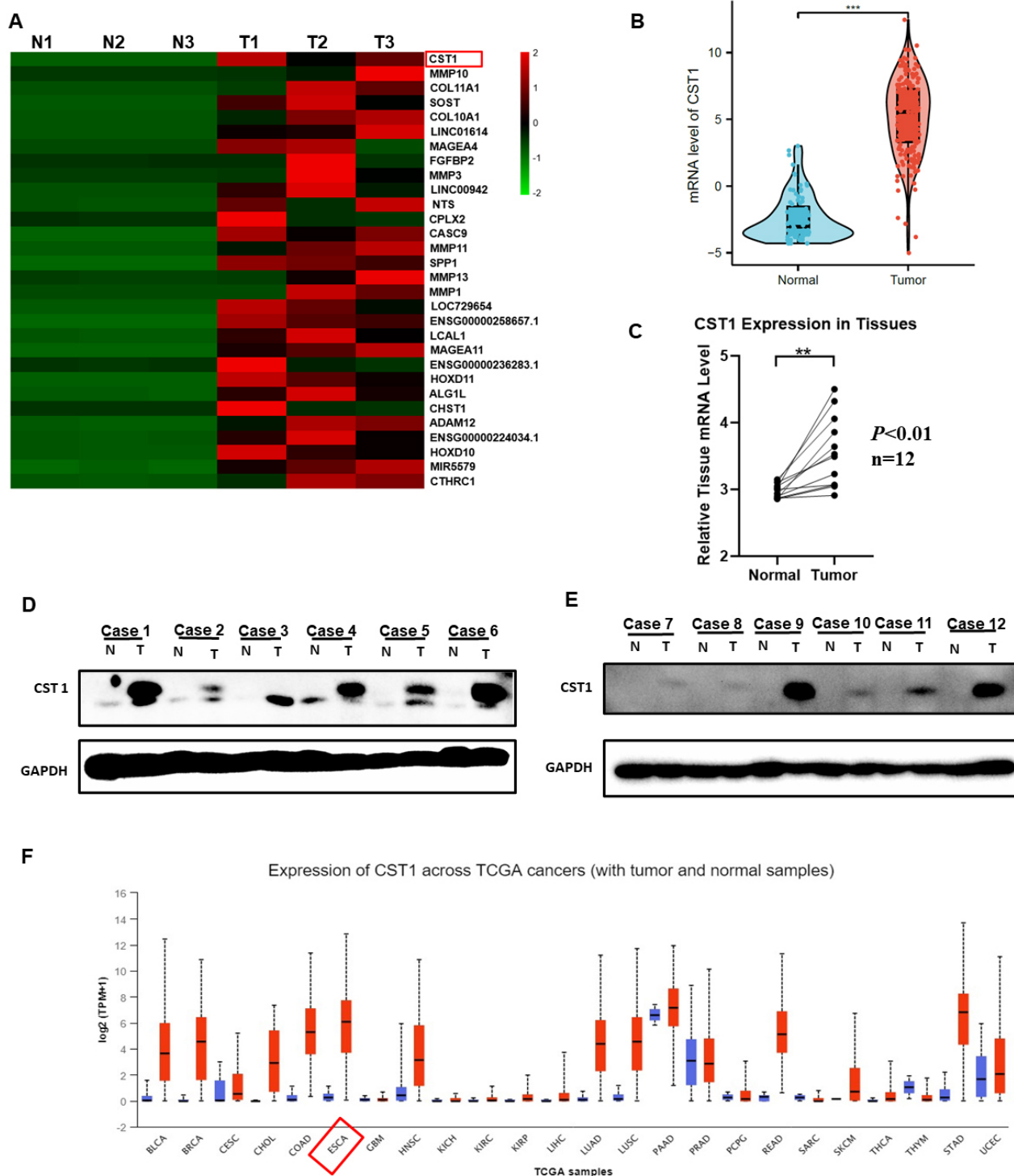
Figure 1

Fig. 1. Cystatin SN (CST1) significantly up-regulated in esophageal squamous cell carcinoma (ESCC). (A) A differential expression heatmap showed the top 25 overexpressed genes in three self-paired ESCC and tumor-adjacent tissues based on the RNA-sequencing. (B) The mRNA level of *CST1* in 180 esophageal cancer (ESCA) and 80 normal tissues in The Cancer Genome Atlas (TCGA) database, $p < 0.001$. (C~E) Relative mRNA and protein level of CST1 in 12 self-paired ESCC and tumor-adjacent tissues were detected by quantitative PCR (qPCR) and western blotting. (F) *CST1* expression level in pan-cancer (in red box) and paired normal tissues (in blue box) and found that CST1 was highly expressed in a variety of tumors, including ESCA based on TCGA database. Data were presented as the mean $\pm$ s.d. of three independent experiments. **$p < 0.01$, ***$p < 0.001$ by student's *t*-test.

Table 2. Correlation of CST1 and clinicopathological parameters in the 220 Formalin-fixed, paraffin-embedded ESCC tissues based on Immunohistochemistry (IHC).

Variables	CST1 expression				
	Cases (%)	Low expression	High expression	χ^2	p value
Age[a]					
≥60	124 (56.4%)	53	71	1.184	0.277
<60	96 (43.6%)	49	47		
Gender					
Male	177 (80.5%)	85	92	0.69	0.406
Female	43 (19.5%)	17	26		
BMI					
BMI <18.5	19 (12.6%)	9	10		
18.5–24	101 (66.9%)	48	53	4.042	0.133
BMI ≥24	31 (20.5%)	21	10		
Smoking status					
No	50 (33.1%)	22	28	1.754	0.185
Yes	101 (66.9%)	56	45		
Alcohol consumption					
No	81 (53.6%)	40	41	0.361	0.548
Yes	70 (46.4%)	38	32		
Family history					
No	135 (89.4%)	72	63	1.436	0.231
Yes	16 (10.6%)	6	10		
Tumour location					
Upper	16 (10.6%)	11	5		
Middle	93 (61.6%)	50	43	4.14	0.126
Lower	42 (27.8%)	17	25		
Differentiation					
Well	24 (15.9%)	12	12		
Moderate	89 (58.9%)	44	45	0.794	0.672
Poor	38 (24.2%)	22	16		
pT status					
T1	12 (5.7%)	7	5		
T2	38 (18%)	18	20	0.745	0.863
T3	153 (72.5%)	70	83		
T4	8 (3.8%)	4	4		
pN status					
N0	104 (49.3%)	60	44		
N1	75 (35.5%)	29	46	11.558	0.009
N2	24 (11.4%)	6	18		
N3	8 (3.8%)	4	4		
TNM stage					
I	23 (11.0%)	13	10		
II	82 (39.0%)	46	36	7.911	0.048
III	100 (47.6%)	37	63		
IV	5 (2.4%)	3	2		
Vascular invasion					
No	121 (80.1%)	65	56	1.038	0.308
Yes	30 (19.9%)	13	17		
Nerve tract invasion					
No	112 (74.2%)	58	54	0.003	0.957
Yes	39 (25.8%)	20	19		

Abbreviations: CI, confident interval; HR, hazard ratio; OR, odds ratio; BMI, Body Mass Index; TNM, T is tumour site and size, N is lymph node involvement, M is distant metastatic spread.
[a] Median age.

ESCC and 19 normal tissue samples. CST1 was mainly expressed in tumor tissues and was absent in normal tissues (Fig. 2A). The median value of the immunohistochemical score was used as the cutoff value, and samples were divided into high and low expression groups. The correlations between CST1 and clinical parameters are shown in Table 2. As shown in Table 2, a total of 118 of 220 (53.64%) ESCC tissue samples exhibited high CST1 expression, while only 2 of 19 (10.53%) normal tissue samples showed high CST1 expression. More importantly, Kaplan–Meier survival analysis was performed to analyze the correlations between the expression of CST1 and clinical parameters, which showed that ESCC patients with higher CST1 expression had significantly shorter overall survival (OS) and disease-free survival (DFS) than ESCC patients with low expression (Fig. 2B,C). Moreover, the results indicated that the expression of CST1 may be correlated with lymph node stage and TNM stage. Survival curves for the entire ESCC patient cohort stratified by combinations of CST1 expression and clinical stage (Fig. 2D) showed that CST1 expression combined with TNM stage (TNM I/II as early-stage ESCC and TNM III/IV as advanced-stage ESCC) could also predict the prognosis of ESCC patients, with high CST1 expression predicting poor outcomes. Additionally, CST1 combined with tumor differentiation yielded similar results (Fig. 2E). Furthermore, high expression of CST1 was associated with dismal OS when combined with tumor size (Fig. 2F) or lymph node stage (Fig. 2G). In addition, advanced lymph node stage tissues had a higher CST1 expression level than normal and early-stage tissues (Fig. 2G). Moreover, univariate and multivariate Cox regression analyses indicated that CST1 expression and lymph node stage could be independent predictors of ESCC prognosis (Table 3). In addition, survival analysis using clinical parameters revealed that most of the parameters had an impact on the OS of ESCC patients, including TNM stage, lymph node stage, tumor size, age, vascular invasion, family history, and body mass index (BMI). To further investigate the prognostic value of CST1 in different clinical parameter subgroups, we analyzed high and low CST1 expression subgroups within different clinical parameters. In the subgroup analyses, high expression of CST1 was still associated with a poorer prognosis for ESCC (Table 3).

Furthermore, we analyzed the relationship between the risk score and patient follow-up time, and data from the 180 samples in TCGA database suggested that high CST1 expression had an impact on increasing the survival time of ESCA patients (Fig. 3A). In addition, high expression of CST1 was closely associated with poor OS in ESCA patients (Fig. 3B, **Supplementary Fig. 1G**). The mRNA expression level of CST1 in advanced clinical stage III/IV disease was higher than that in early stage I/II disease (**Supplementary Fig. 1H**). Data from TCGA indicated that univariate and multivariate Cox regression analyses indi-

cated that CST1 expression, age and clinical stage could be independent predictors of ESCA prognosis (Fig. 3C,D). Hereafter, a nomogram based on these independent prognostic factors was constructed to predict the 1-, 3-, and 5-year survival probability for ESCA patients (Fig. 3E).

3.3 The Transcription Factor SPI1 can Upregulate CST1 mRNA Expression by Binding to the CST1 Promoter

We aimed to explore what causes the upregulation of CST1 in ESCC; thus, we further investigated which transcription factors influence the transcriptional activity of the *CST1* gene. There are many online databases for predicting gene transcription factors, including JASPAR (https://jaspar.genereg.net/), hTFtarget [37], and GTRD [38]. We used the three transcription factor databases described above to predict the specific TF that can upregulate the transcription of the *CST1* gene. The predicted TFs of the three databases intersected; afterward, the results showed that two common transcription factors were obtained, namely, AR (androgen receptor) and SPI1 (Spi-1 proto-oncogene) (Fig. 4A). Because our previous data revealed no significant difference between CST1 and patient sex, we will investigate the effect of another TF, SPI1, on CST1 transcriptional activity. Our previous study demonstrated that AR protein levels were not significantly upregulated in ESCC [39]. In addition, we analyzed the transcription factor-binding sites (TFBS) of SPI1 in the CST1 promoter region in the JASPAR database (Fig. 4B). Simultaneously, SPI1 can directly bind with the SPI1 binding element (SBE) in the CST1 promoter from the transcription start site (TSS), 388 bp upstream of the TSS, and the sequence of SBE was 5′-AGCAAACAGGAAGTCACATA-3′ (Fig. 4C). The SPI1 expression plasmid was transiently transfected into ESCC cell lines Ec109 and K30, and the mRNA expression level of CST1 was then detected by qPCR. The results showed that the mRNA level of CST1 was significantly increased in the Ec109 and K30 SPI1 overexpression groups compared with the control ($t = 13.37$, $p = 0.0055$; $t = 24.15$, $p < 0.001$) (Fig. 4D). A dual-luciferase reporter system was used to study the effect of SPI1 on the transcriptional activity of the CST1 promoter. The results showed that the luciferase fluorescein activity of the cotransfection SPI1 expression plasmid and CST1 promoter luciferase plasmid was significantly higher than only empty vector control cotransfection with the CST1 promoter plasmid ($t = 3.899$, $p = 0.0176$), which means that SPI1 can positively regulate the transcriptional activity of the *CST1* gene (Fig. 4E).

In addition, we know that the expression of CST1 is significantly elevated in ESCC, which may be transcriptionally regulated by SPI1. We further explored SPI1 expression in ESCC and its prognostic value based on bioinformatics analysis. Survival curves showed that a high expression of SPI1 was associated with relatively poor survival in ESCA based on TCGA and GEO databases (Fig. 4F,G). The mRNA level of SPI1 in ESCA was sig-
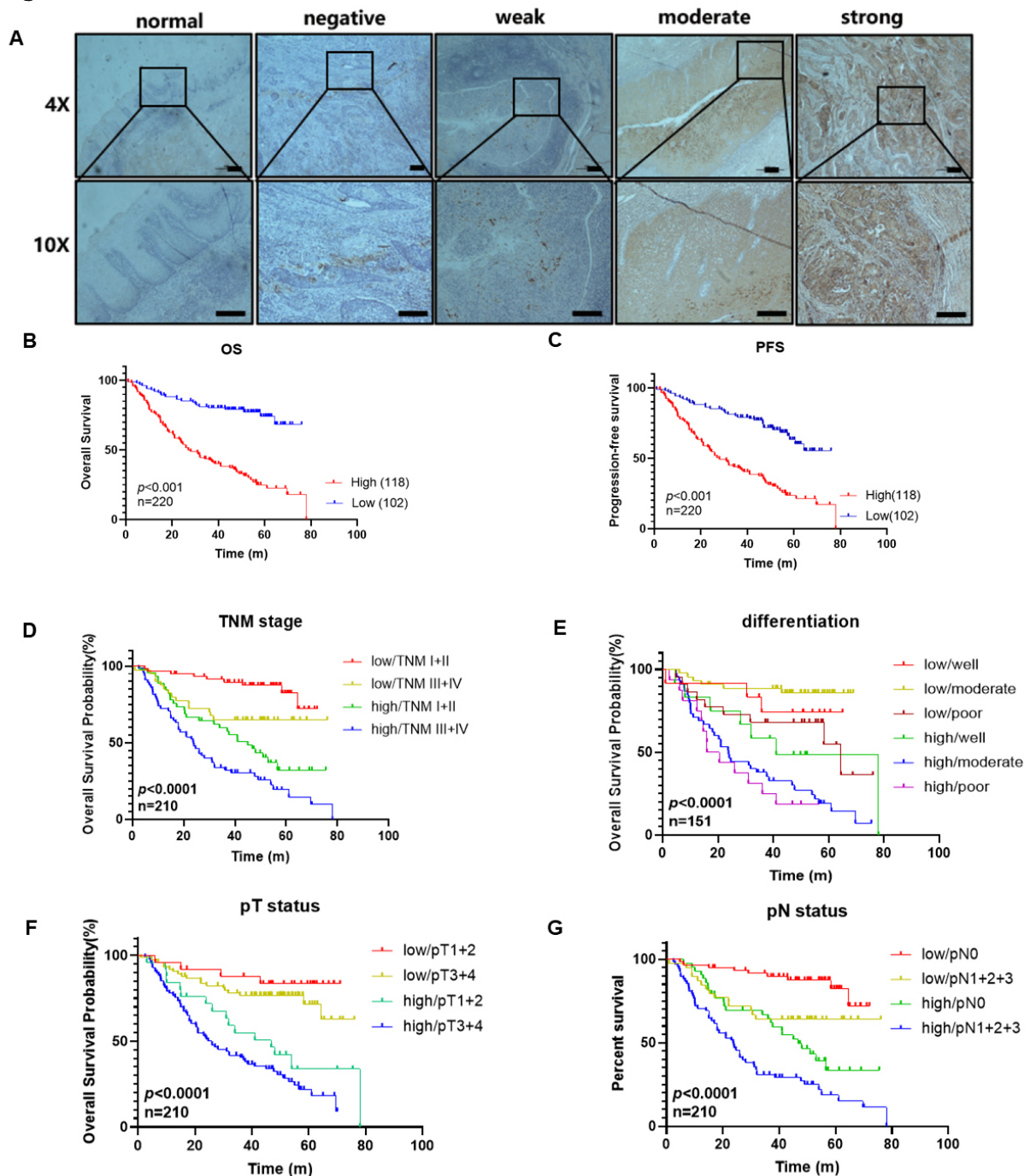
Figure 2

Fig. 2. Up-regulated CST1 was associated with relatively poor survival based on immunochemistry. (A) CST1 was mainly expressed in tumor tissues and rarely absent in normal tissues by Immunohistochemical staining. Negative CST1 staining in normal esophagus epithelium (negative control), negative, weak, moderate and strong staining of CST1 in ESCC cytoplasm, ×100 (4×), ×400 (10×). (B,C) Kaplan-Meier survival analysis showed that ESCC patients with higher CST1 expression had significantly shorter overall survival (OS) and disease-free survival (DFS) than ESCC patients with low expression. (D,E) CST1 expression combined with TNM stage (TNM I/II as early-stage ESCC and TNM III/IV as advanced-stage ESCC) could also predict the prognosis of ESCC patients and high CST1 expression predicting poor outcomes combined with tumor differentiation. (F,G) High expression of CST1 was associated with dismal overall survival when combined with tumor size (2F) or lymph node stage (2G). PFS, progression-free survival; pT for tumour stage; pN for node stage; TNM, tumour-node-metastasis stage.

Table 3. Univariate and multivariate analyses of clinicopathological parameters and CST1 for overall survival in the 220 Formalin-fixed, paraffin-embedded ESCC samples based on IHC.

Variables	Univariate analysis		Multivariate analysis	
	HR (95% CI)	p value	HR (95% CI)	p value
CST1 expression	4.373 (2.771, 6.900)	<0.001	4.94 (2.737, 8.916)	<0.001
Age	1.546 (1.040, 2.297)	0.031	1.353 (0.811, 2.258)	0.246
Gender	0.768 (0.468, 1.261)	0.297	-	-
Differentiation	1.331 (0.926, 1.914)	0.122	-	-
pT status	1.550 (1.081, 2.223)	0.017	1.419 (0.249, 8.105)	0.694
pN status	1.733 (1.412, 2.126)	<0.001	3.434 (1.061, 11.106)	0.039
TNM stage	1.826 (1.349, 2.473)	<0.001	0.484 (0.130, 1.796)	0.278

HR, Hazard ratio; CI, confidence interval.

nificantly higher than that in normal tissue in the TCGA database (Fig. 4H). Further bioinformatics analysis revealed that the mRNA levels of CST1 and SPI1 were positively correlated based on the 180 ESCA samples in TCGA database (r = 0.355, p < 0.001) and the 119 samples in GEO database (r = 0.318, p < 0.001) (Fig. 4I,J).

3.4 Overexpression of CST1 Facilitated Proliferation in Vitro and in Vivo without Inhibiting Apoptotic Death or Cell Cycle Arrest in ESCC Cells

qPCR was used to detect the relative mRNA level and Western blotting was conducted to detect the protein levels of CST1 in 8 ESCC cell lines and one normal immortalized esophageal cell line, NE1 (Fig. 5A,B).

We constructed stable CST1 knockdown cells in Ec109 cells with high CST1 mRNA levels and stable overexpression cells in K510 and K30 cells with low CST1 mRNA levels by stably knocking down CST1-targeted shRNA (knock down 22 and knock down 24; KD22 and KD24) and scrambled shRNA (SCR) as controls and stable overexpression by the CST1 ORF plasmid and its empty vector as a control, respectively. Since CST1 protein is a secreted protein, we detected the concentration of CST1 protein in extracellular conditioned medium (CM) by ELISA to confirm that the stable expression cell construction system was working (Fig. 5C). These stable cell lines were confirmed by real-time qPCR (Fig. 5D–F). Then, MTS assays were performed to test the proliferation ability of tumour cells and we showed that knockdown of CST1 significantly suppressed the proliferation of Ec109 cells compared with the control groups (Fig. 5G). In contrast, the overexpression of CST1 promoted the proliferation of K510 and K30 cells *in vitro* (Fig. 5H,I). The results from colony formation assays further confirmed that CST1 can accelerate tumor proliferation *in vitro* (Fig. 5J–O).

To further investigate whether CST1 affects cell proliferation *in vivo*, the overexpression of CST1 in K30 cells and its control cells was subcutaneously inoculated into BALB/C nude mice (Fig. 5P). The overexpression of CST1 significantly augmented tumor growth *in vivo* compared with that in the control group, and the tumor weight and vol-

ume of the CST1 overexpression group were significantly higher than those of the controls in K30 cells (Fig. 5Q,R). In addition, we examined the cell cycle and early apoptosis in CST1 knockdown and overexpressing stable cell lines by flow cytometry (FCM), and we found no significant difference in early apoptosis. However, we found cell cycle arrest in G0/G1 phase in CST1 stable knockdown cells (**Supplementary Fig. 2A,B,F,H**) with its control. The CST1 stable overexpressing cells (**Supplementary Fig. 2C,D,G,I**) with its control no significant difference in early apoptosis and cell cycle arrest. The cell cycle arrest biomarkers p53 did not seem to be obviously changed and cyclin D1 seems to down-regulated slightly in CST1 knockdown cells by Western blotting (**Supplementary Fig. 2E**).

3.5 Overexpression of CST1 can Promote the Invasion and Migration of ESCC Cells in Vivo and in Vitro

To validate the role of CST1 in ESCC motility, a scratch healing assay was used to assess the regulatory effect of CST1 on migration. The results showed that wound closure occurred gradually 72 h after scratching, whereas this effect on wound healing was significantly reduced after CST1 knockdown in Ec109 cells (Fig. 6A,B) and significantly increased after CST1 overexpression in K30 and K510 cells (Fig. 6F,G; **Supplementary Fig. 2J,K**). The stable knockdown of CST1 in Ec109 cells significantly reduced the migratory (Fig. 6C,D) and invasive (Fig. 6C,E) abilities. Conversely, stable overexpression of CST1 in K510 and K30 cells yielded great enhancement of migration and invasive (Fig. 6H–K; **Supplementary Fig. 2L,M**) abilities compared with the control cells. These results proved that CST1 was involved in promoting migration and invasion.

Epithelial mesenchymal transition (EMT) plays crucial roles in tumor metastasis, and decreasing epithelial biomarkers and/or increasing mesenchymal biomarkers can enhance the motility of tumor cells [40]. We found that CST1 knockdown downregulated the expression of the mesenchymal markers Vimentin and N-cadherin and upregulated that of the epithelial markers E-cadherin and desmoplakin in Ec109 cells by immunoblotting assays. In con-
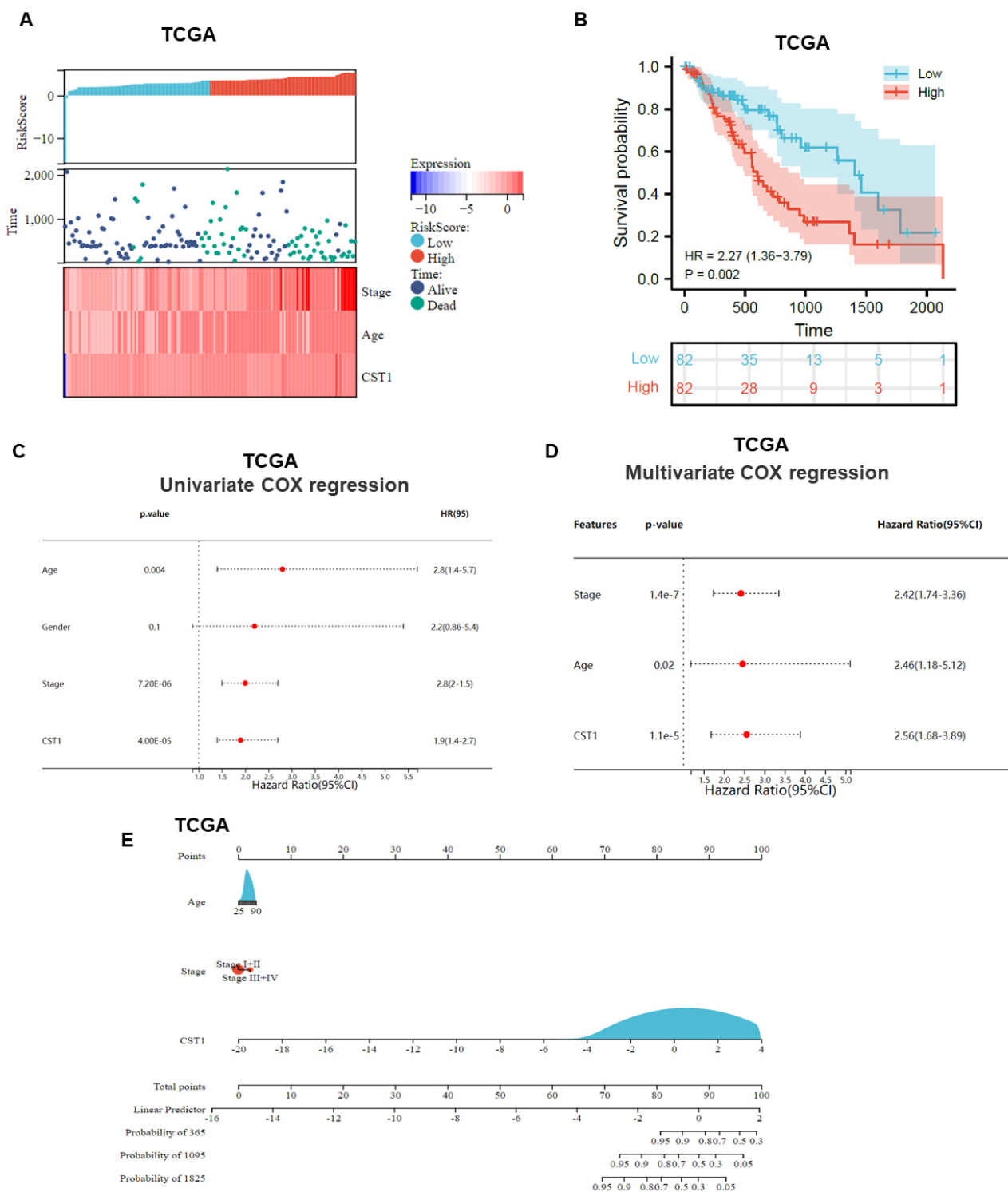
Figure 3

Fig. 3. Up-regulated CST1 was associated with relatively poor survival based on bioinformatics analysis. (A) A model describing the relationship between different risk scores and follow-up time, events, and changes in gene expression in 180 ESCA samples based on TCGA database. (B) Survival curve showed high expression of CST1 was associated with relatively poor survival in ESCA based on TCGA database. (C,D) Data from TCGA indicated that univariate and multivariate Cox regression analyses indicated that CST1 expression, age and clinical stage could be independent predictors of ESCC prognosis. (E) A nomogram was constructed by integrating CST1 expression, age, clinical stage based on 180 ESCA samples in TCGA datasets.
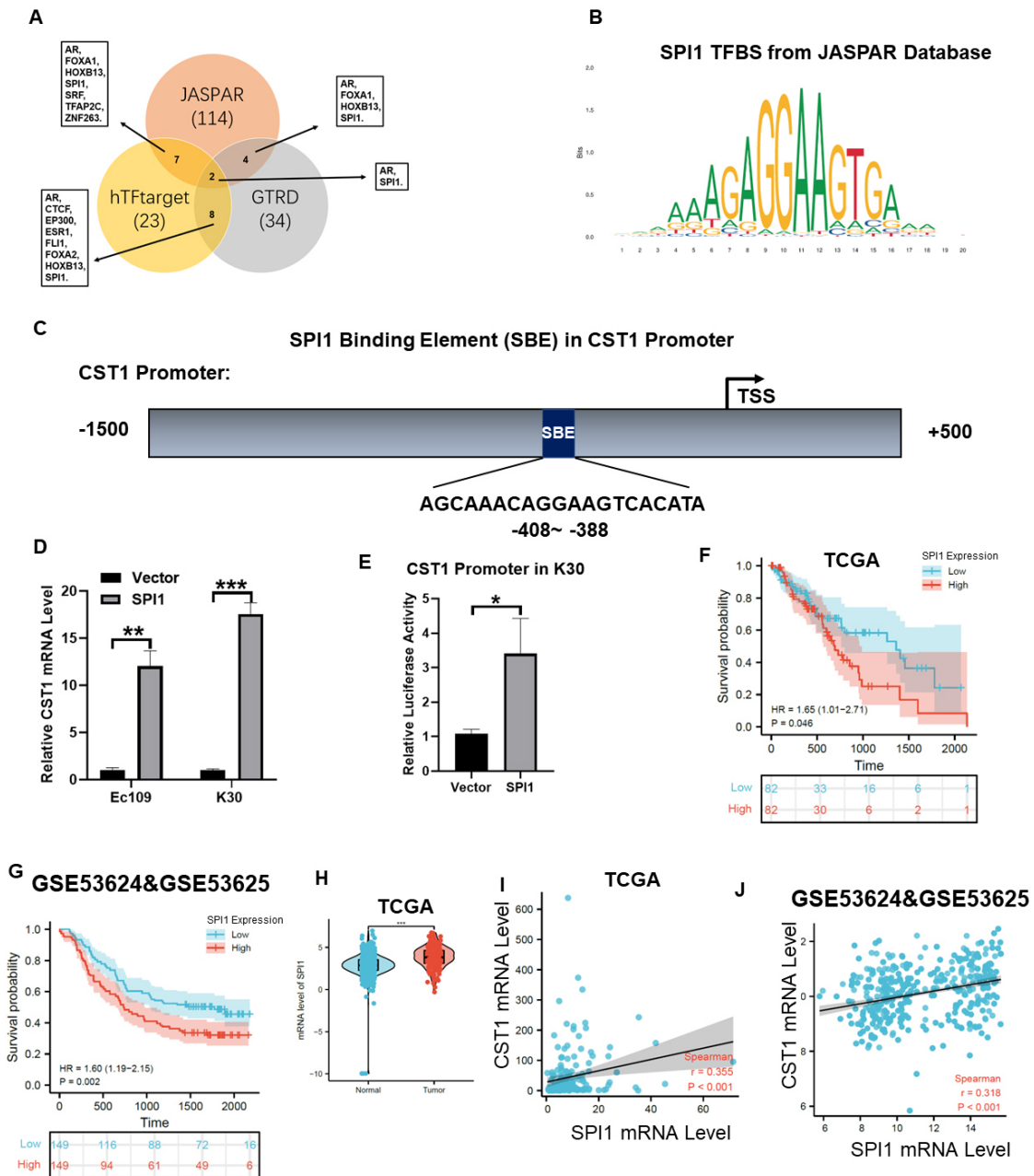
Figure 4

Fig. 4. SPI1 can positively regulate the expression of CST1. (A) Three online databases for predicting gene transcription factors (TF), including JASPAR, hTFtarget and GTRD, were used to predict the TF which can regulate CST1 expression in ESCC. (B) SPI1 was demonstrated as a TF to regulate CST1 expression and its transcription factors binding site (TFBS) in JASPAR database was showed. (C) SPI1 Binding Element (SBE) in CST1 Promoter was 388 bases upstream away from the transcription start site (TSS) in the picture. (D) The mRNA level of CST1 was significantly upregulated in SPI1 overexpressed ESCC cells than in empty vector control. (E) In a dual-luciferase reporter system experiment, CST1 promoter luciferase activity was increased in SPI1 overexpressed ESCC cells than empty vector control. (F,G) Survival curve showed high expression of SPI1 was associated with relatively poor survival in ESCA based on TCGA and GEO database. (H) The mRNA level of SPI1 in ESCA and normal tissue in TCGA database. (I,J) Further bioinformatics analysis revealed that the mRNA level of CST1 and SPI1 was positively correlated based on 180 ESCA samples in TCGA database (r = 0.355, $p < 0.001$) and 119 ESCA samples GEO database (r = 0.318, $p < 0.001$). Data were presented as the mean $\pm$ s.d. of three independent experiments. *$p < 0.05$, **$p < 0.01$, ***$p < 0.001$ by student's *t*-test.
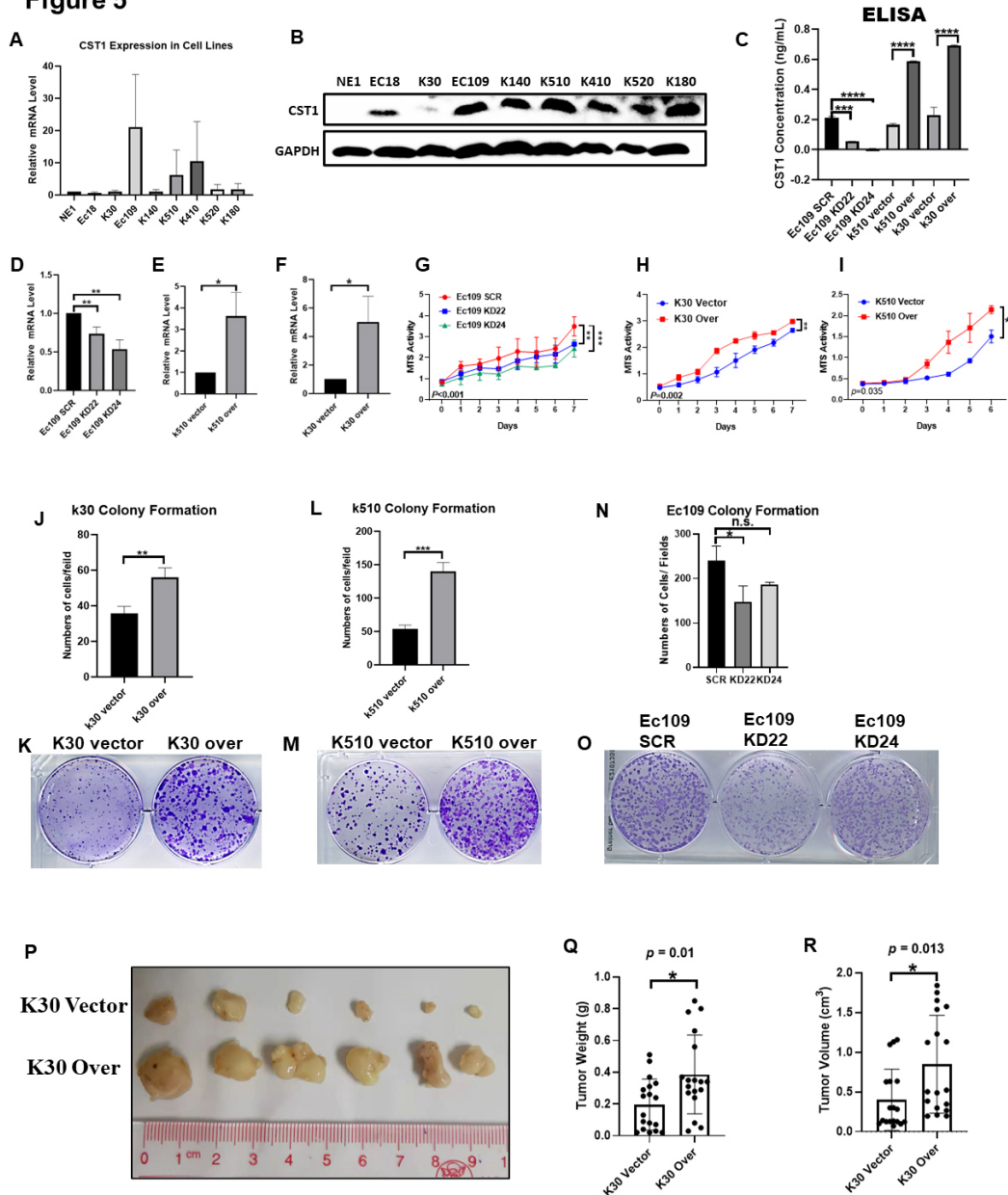
Figure 5

Fig. 5. Over-expression of CST1 facilitated proliferation *in vitro* and *in vivo*. (A,B) Relative mRNA and protein level of CST1 in 8 ESCC cell lines and one normal immortalized esophagus cell line NE1 were detected by qPCR and western blotting. (C–F) We constructed stable CST1 knock-down cells in highly CST1 mRNA level Ec109 cell and stable over-expressed cells in low CST1 mRNA level K510 and K30 cells, by stable knocking down with CST1-targeted shRNA (knock down 22 and knock down 24; KD22 and KD24) and scrambled shRNA (SCR) as controls; and stable over-expression by CST1 ORF plasmid and its empty vector as control, respectively. These stable cell lines confirmed by real-time qPCR and ELISA. (C) We detected the concentration of CST1 protein in extracellular conditioned medium (CM) by Enzyme-Linked Immunosorbent Assay (ELISA) to conform the stable expression cells construction system was working. (G–I) Knockdown of CST1 significantly suppressed the proliferation of Ec109 cells compared to the shSCR control groups by MTS assays (G). By contrast, the overexpression of CST1 promoted the proliferation of K510 and K30 cells (H,I). (J–O) Colony formation assays further verified that CST1 can accelerate the proliferation of ESCC cells. (P) *In vivo* experiment showed CST1 can accelerate the proliferation of ESCC cells, and the stable over-expression of CST1 in K30 cells and its control cells were subcutaneously inoculated into BALB/C nude mice. (Q,R) The over-expression of CST1 could significantly augmented the tumor growth *in vivo* than its control group, and the tumor weight and volume of CST1 over-expression group were significantly higher than controls in K30 cells. Data were presented as the mean ± s.d. of three independent experiments. *$p < 0.05$, **$p < 0.01$, ***$p < 0.001$, ****$p < 0.0001$ by student's *t*-test. MTS for (3-(4,5-Dimethylthiazol-2-yl)-2,5-diphenyltetrazolium bromide).
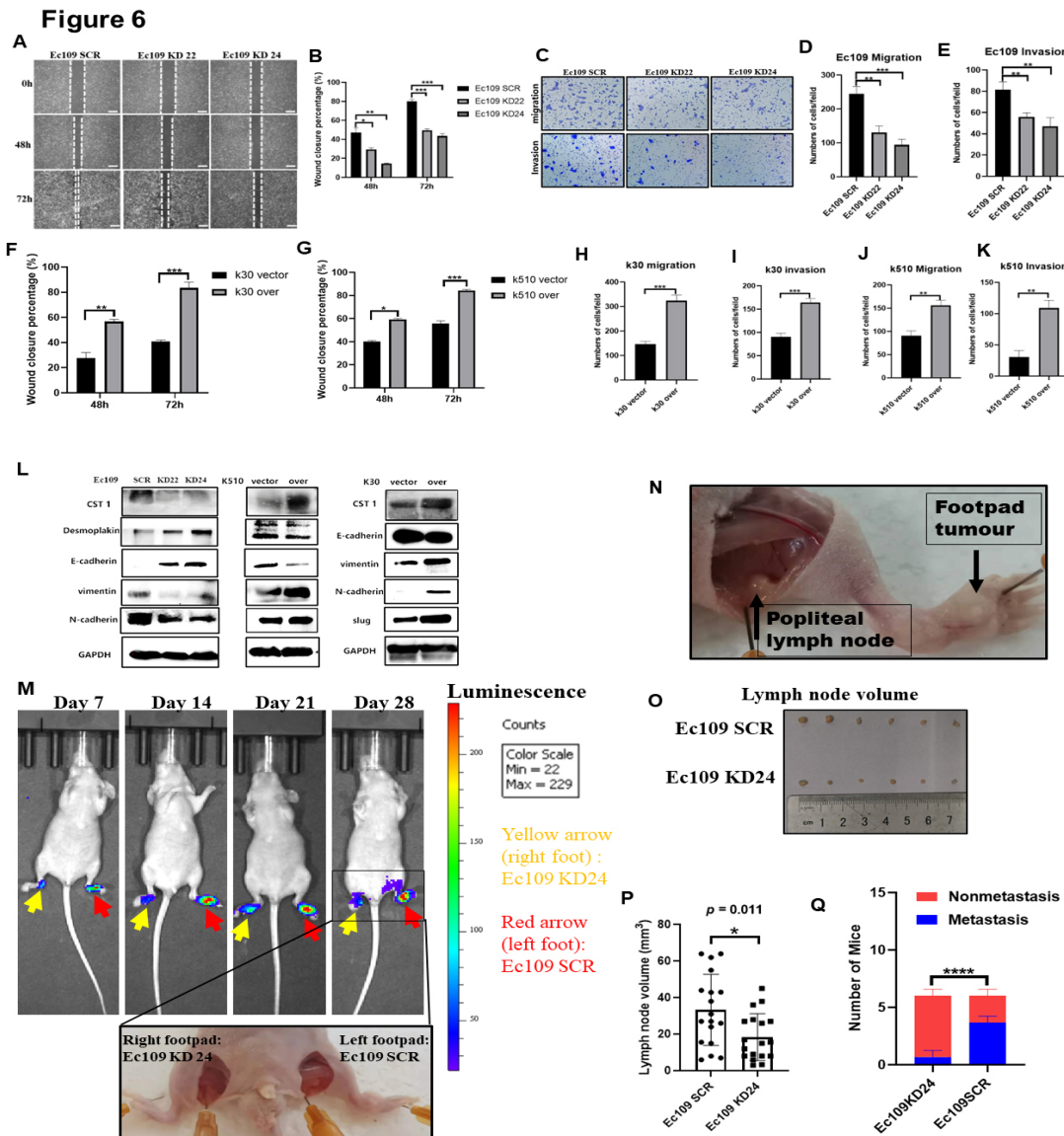
Fig. 6. Overexpressed CST1 can promote invasion and migration of ESCC cells *in vitro* and *in vivo*. (A,B) The scratch healing assay was used to assess the regulation ability of CST1 in migration. The results showed that wound closure occurred gradually 72 h after scratching, whereas this effect of wound healing was significantly reduced after CST1 knockdown in Ec109 cells. (C–E) The stable knocking down CST1 cell Ec109 was significantly reduced the migratory (C,D) and invasive (C,E) abilities. (F–G) The wound healing was significantly increased after CST1 over-expression in K30 and K510 cells. (H–K) Conversely, CST1 stable overexpression in K510 and K30 cells showed great enhancement of migratory and invasive abilities compared with the control cells. CST1 stimulated the EMT and accelerated motility of ESCC cells. (L) CST1 knockdown downregulated the expression of mesenchymal markers Vimentin, N-cadherin, and upregulated that of epithelial markers E-cadherin and Desmoplakin in Ec109 cells by immunoblotting assays. In contrast, overexpressing CST1 in K510 and K30 cells upregulated the expression of Vimentin and N-cadherin and downregulated the expression of E-cadherin and Desmoplakin, as well as that of EMT promoting transcription factors Slug. (N–M) Overexpressed CST1 can promote metastasis of ESCC cells *in vivo*. (O,P) To further explore whether CST1 modulates tumor metastasis *in vivo*, the knockdown CST1 in Ec109 cells were transplanted into nude mice via footpad injection, and we measured the fluorescence intensity of tumors in the mouse feet once a week. After 4 weeks, the results showed a drastically lower rate of popliteal lymph node metastasis in mice injected with the CST1 knockdown cell lines Ec109-KD24 than in those injected with Ec109-SCR cells. (Q) Examination of popliteal lymph node metastasis by measuring lymph node volume and lymph node RNA extraction then running qPCR with using specific primers for human HPRT, which do not cross-react with the corresponding mouse gene. (Q) The result showed that popliteal lymph node metastasis was markedly suppressed after the downregulation of CST1 in Ec109 cells. Data were presented as the mean ± s.d. of three independent experiments. *$p < 0.05$, **$p < 0.01$, ***$p < 0.001$, ****$p < 0.0001$ by student's *t*-test. Min, minimum; Max, maximum.

trast, overexpressing CST1 in K510 and K30 cells upregulated the expression of Vimentin and N-cadherin and downregulated the expression of E-cadherin and desmoplakin, as well as that of the EMT-promoting transcription factor Slug. Taken together, these results indicate that CST1 may stimulate EMT to accelerate the motility of ESCC cells (Fig. 6L).

To further explore whether CST1 modulates tumor metastasis *in vivo*, Ec109 cells with CST1 knockdown were transplanted into nude mice via footpad injection, and the fluorescence intensity of tumors in the mouse feet was measured once a week. After 4 weeks, the results showed a drastically lower rate of popliteal lymph node metastasis in mice injected with the CST1 knockdown cell line Ec109-KD24 than in those injected with Ec109-SCR cells (Fig. 6N,M). Examination of popliteal lymph node metastasis was performed by measuring lymph node volume (Fig. 6O,P) and lymph node RNA extraction and then running qPCR with specific primers for human HPRT, which do not cross-react with the corresponding mouse gene [34]. The results showed that popliteal lymph node metastasis was markedly suppressed after the downregulation of CST1 in Ec109 cells (Fig. 6Q).

3.6 Serum-Secreted CST1 can be a Potentially Noninvasive Early Diagnostic Method for ESCC Patients, and CST1 Neutralizing Antibody Treatment Can Inhibit ESCC Motility

CST1 was found to be highly expressed in ESCC cells and tissues. Thus, we aimed to determine whether serum CST1 levels are consistent with those in cells and tissues. As a secreted protein, to further study the role of CST1 in the ECM, we conducted ELISA analysis of serum samples from 15 volunteers who underwent a physical examination (control) and total 87 ESCC patients. Compared with that of the healthy population, the serum CST1 level of the ESCC patients was distinctly increased (Fig. 7A). Given that the number of serum samples was limited, we observed only that the expression level of CST1 in the serum was significantly associated with age and tumor pathological differentiation ($\chi^2 = 9.079$, $p = 0.004$; and $\chi^2 = 6.566$, $p = 0.038$, respectively). Elderly ESCC patients aged more than 68 years tended to have higher expression of CST1 in the serum, with a high OR of 9.286 (95% CI 1.985, 43.444). The chi-square test or logistic regression was used to test the cross-table data with the OR and 95% confidence interval (CI), and the cutoff value of CST1 was the mean value in the 38 patients' serum samples with clinical parameters (Table 4). The relationships between the expression of CST1 detected by ELISA and clinical parameters are shown in Table 4. More importantly, high expression of CST1 may serve as a potential serum diagnostic marker, as we plotted the receiver operating characteristic (ROC) curve using the ELISA experimental data. The area under the curve (AUC) was 0.9748 ($p < 0.0001$), which had high diagnostic value (Fig. 7B). The ROC curve was constructed to investigate the diagnostic ability of CST1 expression in predicting the OS

of ESCA patients, which showed that CST1 had a high predictive ability for ESCA patient OS (AUC: 0.805 and AUC: 0.802) based on the GEO dataset and TCGA database, respectively (Fig. 7C,D).

We found that CST1 in the ECM may play an important role in the invasive ability of ESCC cells; thus, we conducted an invasion assay by blocking CST1-neutralizing antibody in K30 CST1-overexpressing cells and empty vector control cells. The invasive ability of ESCC cells was significantly inhibited by antibody neutralization of CST1 secreted into the extracellular medium (Fig. 7E,F).

Moreover, two paired stable knockdown or overexpression CST1 cell lines (Ec109 KD24 and its SCR control; K30 overexpression and its empty vector control) were subjected to RNA sequencing. The RNA datasets obtained by RNA sequencing were used for differential analysis to obtain the intersection of genes with significant differences, and further cluster analysis and KEGG and GO analyses were performed. The top 20 GO terms showed that the function of CST1 may be related to the extracellular region (Fig. 7G,H).

3.7 CST1 Accelerated the Motility of ESCC Cells by Downregulating the Quantity and Enzymatic Activity of MMP2

Through in-depth analysis of RNA-sequencing data, we found that CST1 may interact with some members of the MMP family in the reactome, and the top 20 reactome enrichment terms are shown (Fig. 8A). Similarly, gene set enrichment analysis (GSEA) also showed differential gene enrichment in the collagen catabolic process pathway, which was closely related to the function of the MMP family (Fig. 8B).

Therefore, we wanted to explore how CST1 interacts with these MMP family members, so we assessed the MMP1, MMP2, MMP3, MMP9, MMP10 and MMP13 mRNA levels by qPCR in Ec109 KD24 and Ec109 SCR cells and K30 overexpression and K30 vector cells. However, the results showed that CST1 had no apparent effect on the regulation of the mRNA level of these members of the MMP family (Fig. 8C,D). In contrast, the protein levels of the MMP family (MMP1, 2, 3, 10) were positively associated with CST1 protein levels, which decreased in the CST1 knockdown cells and increased in the CST1-overexpressing cells (Fig. 8E). Western blot results indicated that CST1 knockdown decreased the protein levels of MMP2 (pro-form, 72 kDa) and cleaved the MMP10 proform and turn it into the active form.

Further bioinformatics analysis revealed that the mRNA levels of CST1 and MMP2 were positively correlated ($r = 0.428$, $p < 0.001$) (Fig. 8F). Therefore, we assessed the protein levels of CST1 and MMP2 in 87 ESCC patient serum samples by ELISA and found that the protein levels of CST1 and MMP2 in ESCC patient serum were positively correlated ($r = 0.3005$, $p = 0.0044$) (Fig. 8G).
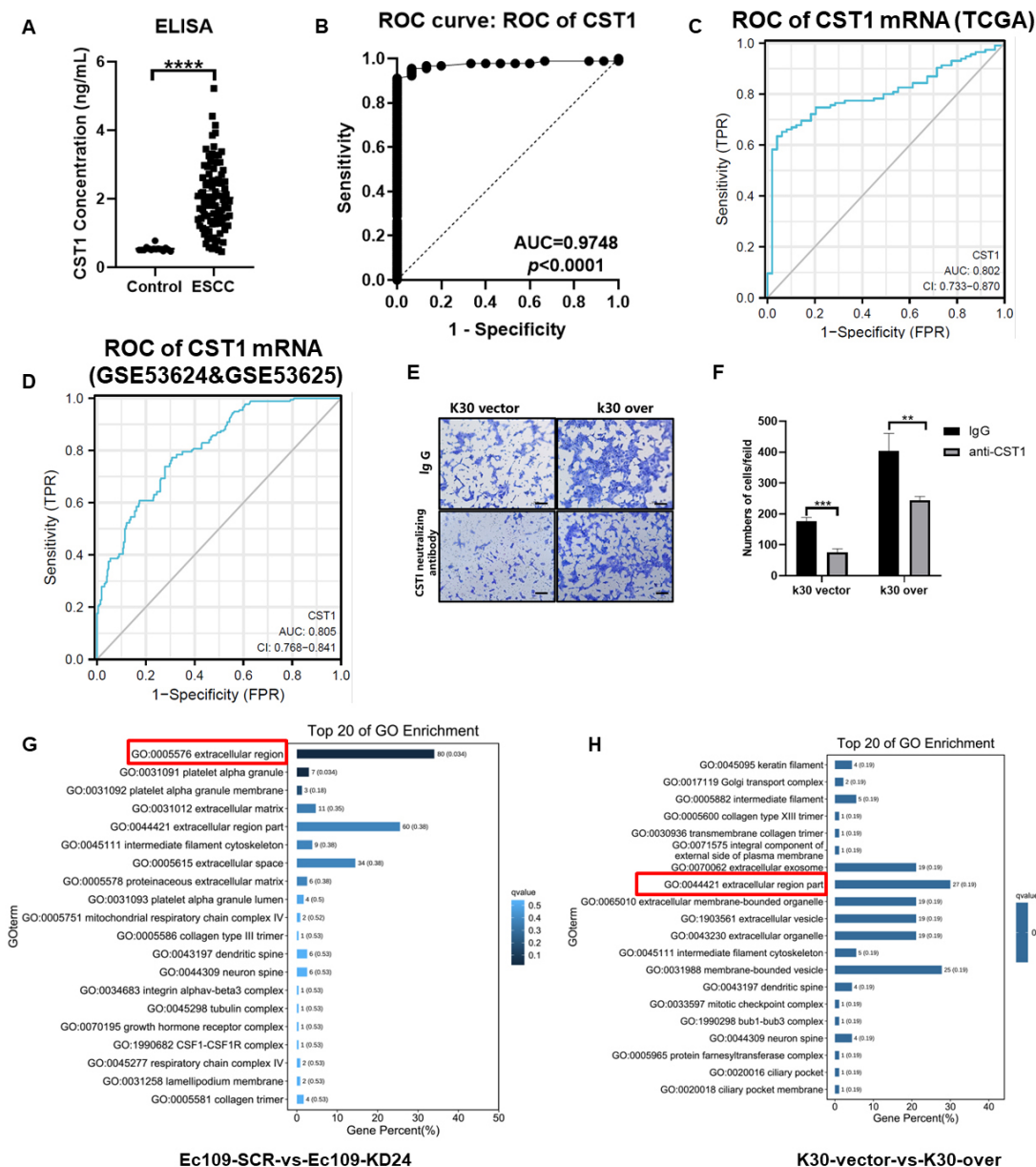
Figure 7

Fig. 7. The serum secreted CST1 can be a potentially non-invasive early diagnostic method for ESCC patients and the new neutralizing antibody drugs target for ESCC treatment. (A) ELISA analysis of CST1 level in serum samples from 15 volunteers who underwent a physical examination (control) and 87 ESCC patients. (B) The area under the curve (AUC) was 0.9748 ($p < 0.0001$), which had high diagnostic value based on ELISA. (C,D) ROC curve was construct to investigate the diagnostic ability of CST1 expression in predicting overall survival of ESCA patients, which showed that CST1 had a high prediction ability of ESCA patient overall survival (AUC: 0.805 and AUC: 0.802) based on the GEO dataset and TCGA database, respectively. (E,F) The invasion assay by CST1 neutralizing antibody blocking in K30 CST1 over-expression and its empty vector control cells. The invasive ability of ESCC cells was significantly inhibited by antibody neutralization of CST1 secreted in the extracellular medium. (G,H) The RNA profiling of two paired stable knockdown or overexpression CST1 cell lines (Ec109 KD24 and its SCR control; K30 over-expression and its empty vector control) obtained by RNA-sequencing was used for differential analysis to obtain the intersection of genes with significant differences, and further cluster analysis, KEGG and GO analysis were performed. The top 20 GO term showed that the function of CST1 may be related to the extracellular region. Data were presented as the mean ± s.d. of three independent experiments. **$p < 0.01$, ***$p < 0.001$, ****$p < 0.0001$ by student's t-test.

Table 4. Correlation of CST1 and clinicopathological parameters in the 38 patients' serum samples based on ELISA assay.

Variables	*CST1* expression					OR 95% CI
	Cases (%)	Low expression	High expression	χ^2	*p* value	
Age						
≥68	20 (52.6%)	7	13	9.079	0.004	9.286 (1.985, 43.444)
<68	18 (47.4%)	15	3			
Gender						
Male	22 (57.9%)	13	9	0.031	1	1.123 (0.305, 4.135)
Female	16 (42.1%)	9	7			
Differentiation						
Well	1 (2.6%)	1	0			
Moderate	28 (73.7%)	19	9	6.566	0.038	0.947 (0.029, 30.942)
Poor	9 (23.7%)	2	7			7.000 (0.166, 294.934)
pT status						
T0	3 (7.5%)	2	0			
T1	5 (12.5%)	4	0	1.751	0.626	0.500 (0.007, 35.820)
T2	8 (20.0%)	4	4			4.000 (0.134, 119.230)
T3	24 (60%)	12	12			4.000 (0.163, 98.190)
pN status						
N0	18 (47.4%)	10	8			
N1	14 (36.8%)	9	5	0.428	0.807	0.694 (0.165, 2.917)
N2	6 (15.8%)	3	3			1.250 (0.196, 7.956)
TNM stage						
0	23 (11.0%)	2	0			
I	82 (39.0%)	3	0	1.71	0.635	0.667 (0.009, 49.575)
II	100 (47.6%)	6	8			5.333 (0.202, 140.997)
III	5 (2.4%)	11	8			2.909 (0.115, 73.543)

We aimed to further investigate whether the CST1 proteins immunoprecipitated MMP2 in the ECM. We conducted immunoprecipitation (IP) experiments with a CST1 antibody and IgG control, and the IP samples were then subjected to SDS gel electrophoresis (Fig. 9A). We found that CST1 immunoprecipitated the band between molecular weights 65 and 75 kDa, which we suspect may be MMP2, as CST1 cleaves the MMP2 pro-form (72 kDa) to generate the MMP2 active form (62 kDa). Therefore, we sent the two IP samples (CST1 and IgG samples) for mass spectrometry to identify which proteins could be specifically immunoprecipitated by CST1. The mass spectrometry results are shown in the table, in which MMP2 can be immunoprecipitated specifically by CST1 (Fig. 9B,C). The coimmunoprecipitation (Co-IP) method was further used to verify that both CST1 and MMP2 physically bind to each other in Ec109 cells (Fig. 9D). We were curious about what role CST1 could play when physically combined with MMP2. Could CST1, a cysteine protease inhibitor, regulate the activity of MMP2 gelatinase? We therefore chose to perform gelatin zymography experiments to further validate the effect of CST1 on the activity of MMP2 gelatinase (Fig. 9E) [32]. Through the zymography assay, we found that CST1 can positively regulate the activity of MMP2 gelatinase. Knockdown of CST1 decreased MMP2 activities, while overexpression of CST1 increased MMP2 activity but had

no obvious effect on the activity of MMP9 (Fig. 9E). The diagram shows that the transcription factor SPI1 upregulates the expression of the CST1 protein at the transcriptional level by binding to the *CST1* gene promoter such that the expression level of the CST1 protein is increased, and the level of secreted CST1 protein is increased in the ECM. The CST1 protein can bind MMP2 and convert precursor MMP2 (pro-MMP2) into active MMP2 protein, leading to the decomposition of gelatin and remodeling of the ECM and further promoting the metastatic ability of ESCC cells (Fig. 9F).

4. Discussion

In this study, we observed that CST1 was highly expressed in 87 ESCC patient serum samples compared with 15 healthy control serum samples based on ELISA. The ROC curve was generated to evaluate the diagnostic significance of the high expression of CST1 in the serum of ESCC patients; interestingly, CST1 can be used as a good diagnostic marker. Consistent with our study, some recent studies reported that CST1 could serve as a serological biomarker for the early diagnosis of ESCC [41], colorectal cancer [15], pancreatic cancer [20], and stomach cancer [42].

The current research on CST1 in ESCA seems to be contradictory. However, we found that upregulated CST1 can be an independent prognostic factor in ESCC, and the
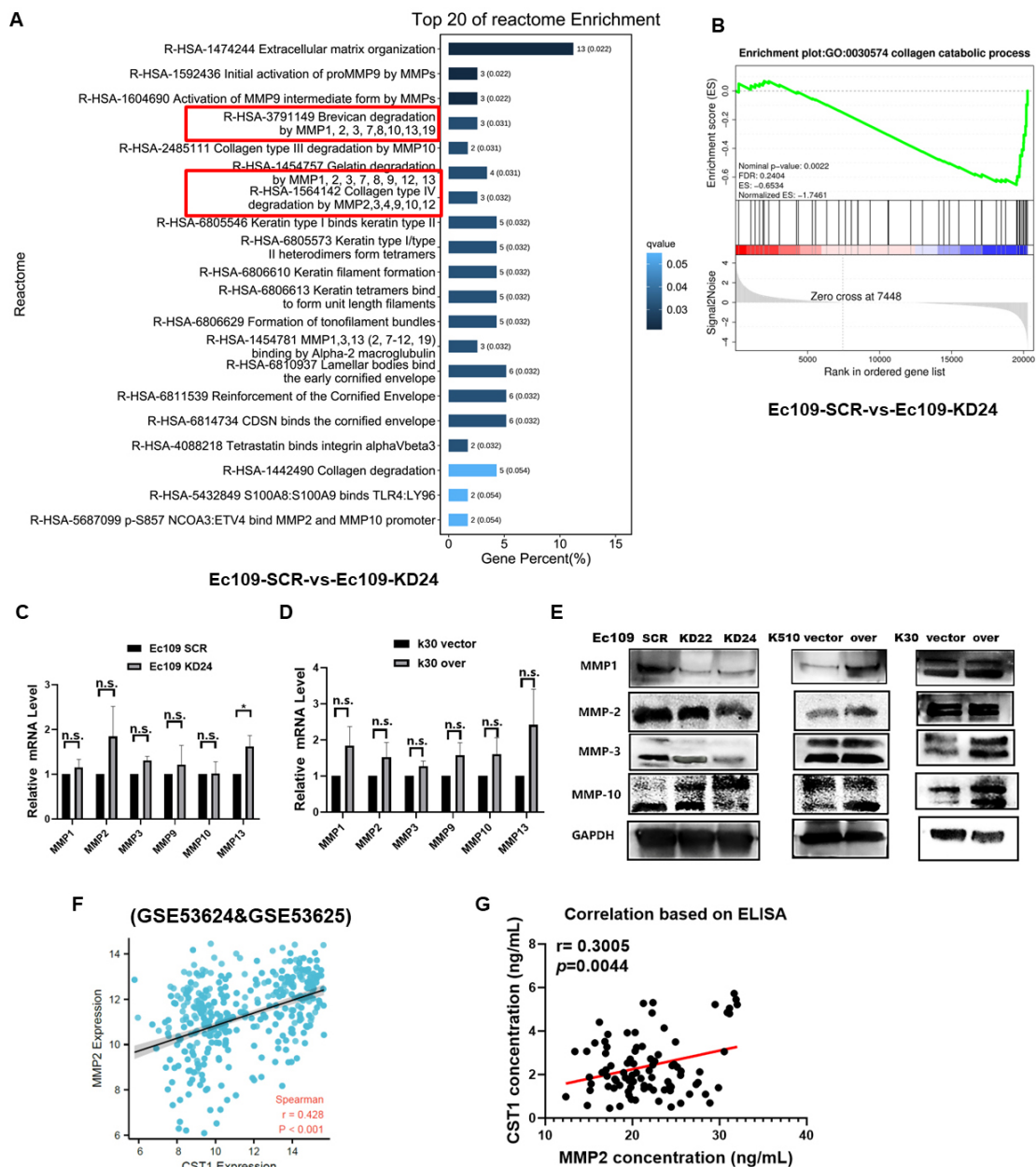
Figure 8

Fig. 8. CST1 accelerated motility of ESCC cells by interacting with matrix metalloproteinase (MMP) family proteins. (A) The top 20 reactome enrichment terms were showed CST1 may interact with some members of the MMP family in reactome based on RNA-sequencing. (B) Gene Set Enrichment Analysis (GSEA) analysis also showed differential gene enrichment in collagen catabolic process pathway, which was closely related to the function of the MMP family. (C,D) We want to explore how CST1 interact with these MMP family members gene, then we detected the MMP1, MMP2, MMP3, MMP9, MMP10 and MMP13 mRNA level by qPCR in Ec109 KD24 & Ec109 SCR cells and K30 over & K30 vector cells. However, the results showed that CST1 had no apparent effect on regulation the mRNA level of these members of the MMP family. (E) The protein levels of the MMP family (MMP1, 2, 3, 10) were positively associated with CST1 protein level, they decreased in the CST1 knock-down cells and increased in the CST1 over-expressed cells. (F) Further bioinformatics analysis revealed that the mRNA level of CST1 and MMP2 was positively correlated ($r = 0.428$, $p < 0.001$) based on GEO database. (G) The CST1 and MMP2 protein level of the 87 ESCC patient serum by ELISA, and it turn out that the protein level of CST1 and MMP2 in ESCC patient serum was positively correlation ($r = 0.3005$, $p = 0.0044$). Data were presented as the mean $\pm$ s.d. of three independent experiments. n.s. : not statistically significant, *$p < 0.05$, by student's t-test.
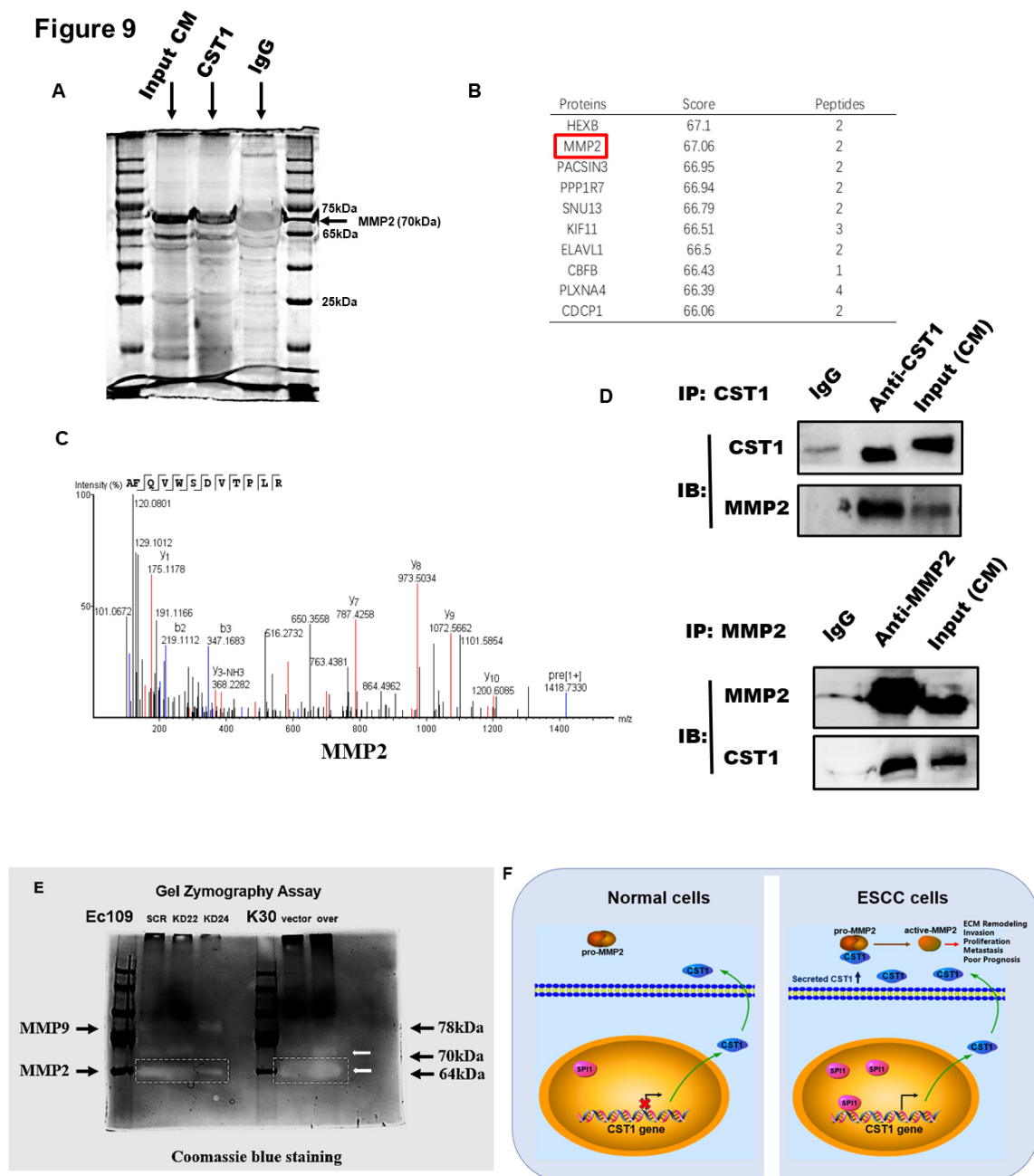
Fig. 9. CST1 accelerated motility of ESCC cells by up-regulating the quantity and enzymatic activity of MMP2. (A) To further investigate whether the proteins of CST1 and MMP2 directly bind in the ECM. Then We conducted the immunoprecipitation (IP) experiments by CST1 antibody and IgG control, and then the IP samples were subjected to run the SDS gel electrophoresis (Coomassie blue staining). (B,C) We sent the two IP samples (CST1 and IgG samples) for mass spectrometry identification to see which proteins could be specifically immunoprecipitated by CST1. The result of mass spectrometry showed in the table, in which MMP2 can be immunoprecipitated specifically by CST1. (D) The co-immunoprecipitation (CO-IP) method was further used to verify that both CST1 and MMP2 bind to each other in Ec109 cells. (E) The gelatin zymography experiments were used to further validate the effect of CST1 on the activity of MMP2 gelatinase, and found CST1 acts as an activator of MMP2. (F) Diagram showed that the transcription factor SPI1 up-regulates the expression of CST1 protein at the transcriptional level by binding to the *CST1* gene promoter, so that the expression level of CST1 protein is increased, and the level of secreted CST1 protein in the is increased in the extracellular matrix (ECM). The CST1 protein can bind MMP2 and convert precursor MMP2 (pro-MMP2) into active MMP2 protein, leading to decompose gelatin and remodel the extracellular matrix, and further promote the metastatic ability of ESCC cells.

high expression of CST1 was associated with an unfavorable prognosis in ESCC, which was consistent with the results for CST1 in many other cancers [14–16,22,23]. Our findings were based on solid basic research and consistent with the results of open database research. Therefore, it is reasonable to conclude that CST1 acts as an oncogene in ESCC. Moreover, our findings highlighted that the expression of CST1 may be correlated with lymph node stage and TNM stage, which indicated involvement in tumor metastasis and malignant progression. One study reported that CST1 was also identified as a novel mediator of bone metastasis by global secretome analysis. Apart from the lymph nodes, the bone is one of the most common sites of distant metastasis by solid tumors [43]. However, there was no evidence that ESCC bone metastasis could be promoted by the high expression of CST1.

It is unclear what causes the upregulation of CST1 in ESCC. Therefore, we used three online databases to further predict some transcription factors that may regulate the transcriptional activity of CST1, and we found that the transcriptional activity of CST1 may be regulated by the transcription factor AR or SPI1. Because our previous data revealed no significant difference between CST1 and patient sex and that AR protein levels were not significantly upregulated in ESCC [39], we investigated the effect of another transcription factor, SPI1, on CST1 transcriptional activity. SPI1 is transcription factor located in nuclear, and its ETS-domain C binds to a purine-rich sequence known as the PU-box found near the promoters of target genes and regulates their expression in coordination with other transcription factors and cofactors (NCBI website). Previous studies indicate that upregulated SPI1 is associated with poor prognosis in breast carcinoma [44], while SPI1 inhibits invasion of hepatocellular carcinoma cells by suppressing insulin-like growth factor 2 expression [45]. Early studies showed that SPI1 was highly expressed in ESCA and was associated with poor prognosis [46,47]. However, SPI1 can also be secreted by immune cells in the ECM and transferred to tumor cells in the form of exosomes to regulate tumor cell gene transcription. Upregulation of SPI1 was found to be associated with poor prognosis in patients suffering from colon cancer [48].

In the current study, our data demonstrated that transcription factor-elevated SPI1 can positively upregulate the transcriptional activity of the *CST1* gene. We suspected that SPI1 may bind to an element (388 bases upstream of the transcription start site) of the CST1 promoter region, but more experiments are needed to validate this hypothesis.

Using a variety of detection methods, we verified that CST1 is highly expressed in ESCC rather than normal tissue and acts as not only a potential biomarker for the early diagnosis of ESCC patients but also an independent predictor of poor prognosis in ESCC patients. CST1 is of practical importance in imparting an aggressive phenotype in ESCC cells, promoting cell proliferation and metastasis *in vitro* and *in vivo*, by contributing to epithelial-mesenchymal transition (EMT) and ECM remodeling. EMT plays crucial roles in tumor metastasis, and decreasing epithelial biomarkers and/or increasing mesenchymal biomarkers can enhance the motility of tumor cells [40].

The transition from the epithelial to mesenchymal phenotype results in reduced expression of epithelial markers, such as E-cadherin and desmoplakin, and increased expression of mesenchymal markers, such as vimentin, N-cadherin, and slug, contributing to cancer cell invasion and metastasis [49].

The TME plays a key role in the development and progression of ESCA and is composed of diverse cellular components, including not only cancer cells but also fibroblasts, immune cells and endothelial cells. Furthermore, one of the most important components of the TME is the ECM, including cytokines, glycoproteins, and glycosaminoglycans that surround tumor cells [50,51].

Type I collagen has been shown to be upregulated in tumors, where it functions to fill the gaps between cancer cells and increase their stiffness, tensile strength and resistance to deformation [52,53]. The tumor cells need biochemical and mechanical support from the collagen and gelatin network in ECM and also need degrade and remodel ECM for tumor progression and invasion. The MMP family is characterized by multidomain zinc-dependent endopeptidases and represents one of the major enzyme classes involved in ECM remodeling, whereas tumor cell-secreted MMPs are a very important feature that promote cancer invasion and dissemination [50,54]. We found CST1-activated MMP2 mediates ECM degradation, a critical step for ESCC cell invasion and metastasis that is associated with a poor clinical outcome in ESCC patients. Another interrelated study showed upregulation of MMP14, which in turn activated MMP2, leading to the degradation of the ECM and increased invasion of ESCA cells [55].

In this study, we found that CST1 is associated with multiple members of the MMP family. Up- or downregulated CST1 could increase or decrease the protein levels of MMP1, MMP2, MMP3, and MMP10 in ESCC cells but did not significantly change the corresponding gene levels. We also identified that CST1 and MMP2 can physically bind to each other by means of mass spectrometry and coimmunoprecipitation in the ECM. At the same time, we further found that upregulated CST1 significantly promoted the enzymatic activity of MMP2 and increased the motility ability of ESCC, which means that CST1 could be an activator of MMP2. Taken together, our study further confirmed that CST1 participates in ECM remodeling and promotes ESCC metastasis in the TME by regulating the activity of MMP2. However, our study was limited to CST1 secreted by tumor cells, and other studies suggested that CST1 secreted by other cellular components in the tumor microenvironment, such as fibroblasts, also had important prognostic significance [56]. In agreement with our data, a

single-cell sequencing-based study reported that a specific population of CST1$^+$ myofibroblasts was characterized by high activities in ECM remodeling, protein secretion, EMT, and TGF-beta pathways. CST1$^+$ fibroblasts were generally much higher in ESCC tumor stromal than in nonmalignant samples and exhibited prominent prognostic values [56]. However, further study is still required to confirm our findings.

5. Conclusions

The upregulated CST1, mediated by SPI1 in the promoter, can be a potentially prognostic biomarker and act as an oncogene in ESCC, which causes ECM remodeling and accelerates ESCC cell invasion and metastasis *in vitro* and *in vivo* by interacting with MMP2.

Consent for Publication

Not applicable.

Availability of Data and Materials

Raw data of this study have been deposited to the Research Data Deposit database (https://www.researchdata.org.cn/) under accession number: RDDB2023563045.

Author Contributions

FFL, JW and ZFZ performed most of in vitro assays. BJH designed the research study. CFY participated in the design of the project and collected paired samples of esophageal cancer and tumor-adjacent normal control. CFY also draft and revise the paper. BQL and MLF performed the statistics analysis. STL and TJH provided help in collecting patient samples and advice on the ELISA experiments and IHC. LXP and STZ preformed the in vivo assay and bioinformatics analysis. All authors contributed to editorial changes in the manuscript. All authors read and approved the final manuscript. All authors have participated sufficiently in the work and agreed to be accountable for all aspects of the work.

Ethics Approval and Consent to Participate

We obtained the human tissue research ethics approval document approved by the Ethics Committee of Sun Yat-sen University Cancer Center, and obtained the consent of the patients to participate. The ethics approval number is: SZR2021-068.

Acknowledgment

Not applicable.

Funding

Conflict of Interest

The authors declare no conflict of interest.

Supplementary Material

Supplementary material associated with this article can be found, in the online version, at https://doi.org/10.31083/j.fbl2809212.

References

[1] Bray F, Ferlay J, Soerjomataram I, Siegel RL, Torre LA, Jemal A. Global cancer statistics 2018: GLOBOCAN estimates of incidence and mortality worldwide for 36 cancers in 185 countries. CA: A Cancer Journal for Clinicians. 2018; 68: 394–424.

[2] Torre LA, Bray F, Siegel RL, Ferlay J, Lortet-Tieulent J, Jemal A. Global cancer statistics, 2012. CA: A Cancer Journal for Clinicians. 2015; 65: 87–108.

[3] Abnet CC, Arnold M, Wei WQ. Epidemiology of Esophageal Squamous Cell Carcinoma. Gastroenterology. 2018; 154: 360–373.

[4] Lagergren J, Smyth E, Cunningham D, Lagergren P. Oesophageal cancer. Lancet (London, England). 2017; 390: 2383–2396.

[5] Diakowska D. Cytokines association with clinical and pathological changes in esophageal squamous cell carcinoma. Disease Markers. 2013; 35: 883–893.

[6] Li Z, Qian J, Li J, Zhu C. Clinical Significance of Serum Chemokines in Esophageal Cancer. Medical Science Monitor: International Medical Journal of Experimental and Clinical Research. 2019; 25: 5850–5855.

[7] Oh SS, Park S, Lee KW, Madhi H, Park SG, Lee HG, *et al*. Extracellular cystatin SN and cathepsin B prevent cellular senescence by inhibiting abnormal glycogen accumulation. Cell Death & Disease. 2017; 8: e2729.

[8] Liu Y, Yao J. Research progress of cystatin SN in cancer. OncoTargets and Therapy. 2019; 12: 3411–3419.

[9] Dickinson DP, Thiesse M, Hicks MJ. Expression of type 2 cystatin genes CST1-CST5 in adult human tissues and the developing submandibular gland. DNA and Cell Biology. 2002; 21: 47–65.

[10] Turk V, Turk B, Turk D. Lysosomal cysteine proteases: facts and opportunities. The EMBO Journal. 2001; 20: 4629–4633.

[11] Hirai K, Yokoyama M, Asano G, Tanaka S. Expression of cathepsin B and cystatin C in human colorectal cancer. Human Pathology. 1999; 30: 680–686.

[12] Koblinski JE, Ahram M, Sloane BF. Unraveling the role of proteases in cancer. Clinica Chimica Acta; International Journal of Clinical Chemistry. 2000; 291: 113–135.

[13] Barrett AJ. The cystatins: a diverse superfamily of cysteine peptidase inhibitors. Biomedica Biochimica Acta. 1986; 45: 1363–1374.

[14] Cao X, Li Y, Luo RZ, Zhang L, Zhang SL, Zeng J, *et al*. Expression of Cystatin SN significantly correlates with recurrence, metastasis, and survival duration in surgically resected non-small cell lung cancer patients. Scientific Reports. 2015; 5: 8230.

[15] Yoneda K, Iida H, Endo H, Hosono K, Akiyama T, Takahashi H, *et al*. Identification of Cystatin SN as a novel tumor marker for colorectal cancer. International Journal of Oncology. 2009; 35: 33–40.

[16] Kim JT, Lee SJ, Kang MA, Park JE, Kim BY, Yoon DY, *et al*. Cystatin SN neutralizes the inhibitory effect of cystatin C on cathepsin B activity. Cell Death & Disease. 2013; 4: e974.

[17] Jiang J, Liu HL, Tao L, Lin XY, Yang YD, Tan SW, *et al*. Let 7d inhibits colorectal cancer cell proliferation through the CST1/p65 pathway. International Journal of Oncology. 2018; 53: 781–790.

[18] Zhou X, Wang X, Huang K, Liao X, Yang C, Yu T, *et al*. Investigation of the clinical significance and prospective molecular mechanisms of cystatin genes in patients with hepatitis B virus related hepatocellular carcinoma. Oncology Reports. 2019; 42: 189–201.

[19] Cui Y, Sun D, Song R, Zhang S, Liu X, Wang Y, *et al*. Upregulation of cystatin SN promotes hepatocellular carcinoma progression and predicts a poor prognosis. Journal of Cellular Physiology. 2019; 234: 22623–22634.

[20] Jiang J, Liu HL, Liu ZH, Tan SW, Wu B. Identification of cystatin SN as a novel biomarker for pancreatic cancer. Tumour Biology: the Journal of the International Society for Oncodevelopmental Biology and Medicine. 2015; 36: 3903–3910.

[21] Choi EH, Kim JT, Kim JH, Kim SY, Song EY, Kim JW, *et al*. Upregulation of the cysteine protease inhibitor, cystatin SN, contributes to cell proliferation and cathepsin inhibition in gastric cancer. Clinica Chimica Acta; International Journal of Clinical Chemistry. 2009; 406: 45–51.

[22] Liu Y, Ma H, Wang Y, Du X, Yao J. Cystatin SN Affects Cell Proliferation by Regulating the ERα/PI3K/AKT/ERα Loopback Pathway in Breast Cancer. OncoTargets and Therapy. 2019; 12: 11359–11369.

[23] Dai DN, Li Y, Chen B, Du Y, Li SB, Lu SX, *et al*. Elevated expression of CST1 promotes breast cancer progression and predicts a poor prognosis. Journal of Molecular Medicine (Berlin, Germany). 2017; 95: 873–886.

[24] Chen YF, Ma G, Cao X, Luo RZ, He LR, He JH, *et al*. Overexpression of cystatin SN positively affects survival of patients with surgically resected esophageal squamous cell carcinoma. BMC Surgery. 2013; 13: 15.

[25] Zhang H, Shi Q, Yang Z, Wang K, Zhang Z, Huang Z, *et al*. An Extracellular Matrix-Based Signature Associated with Immune Microenvironment Predicts the Prognosis and Therapeutic Responses of Patients With Oesophageal Squamous Cell Carcinoma. Frontiers in Molecular Biosciences. 2021; 8: 598427.

[26] Groblewska M, Siewko M, Mroczko B, Szmitkowski M. The role of matrix metalloproteinases (MMPs) and their inhibitors (TIMPs) in the development of esophageal cancer. Folia Histochemica et Cytobiologica. 2012; 50: 12–19.

[27] Zhu YH, Fu L, Chen L, Qin YR, Liu H, Xie F, *et al*. Downregulation of the novel tumor suppressor DIRAS1 predicts poor prognosis in esophageal squamous cell carcinoma. Cancer Research. 2013; 73: 2298–2309.

[28] Zou S, Yang J, Guo J, Su Y, He C, Wu J, *et al*. RAD18 promotes the migration and invasion of esophageal squamous cell cancer via the JNK-MMPs pathway. Cancer Letters. 2018; 417: 65–74.

[29] Adachi Y, Itoh F, Yamamoto H, Matsuno K, Arimura Y, Kusano M, *et al*. Matrix metalloproteinase matrilysin (MMP-7) participates in the progression of human gastric and esophageal cancers. International Journal of Oncology. 1998; 13: 1031–1035.

[30] Chen Y, Wang D, Peng H, Chen X, Han X, Yu J, *et al*. Epigenetically upregulated oncoprotein PLCE1 drives esophageal carcinoma angiogenesis and proliferation via activating the PI-PLCε-NF-κB signaling pathway and VEGF-C/ Bcl-2 expression. Molecular Cancer. 2019; 18: 1.

[31] Li J, Zhang N, Song LB, Liao WT, Jiang LL, Gong LY, *et al*. Astrocyte elevated gene-1 is a novel prognostic marker for breast cancer progression and overall patient survival. Clinical Cancer Research: an Official Journal of the American Association for Cancer Research. 2008; 14: 3319–3326.

[32] Cai HP, Wang J, Xi SY, Ni XR, Chen YS, Yu YJ, *et al*. Tenascin-cmediated vasculogenic mimicry formation via regulation of MMP2/MMP9 in glioma. Cell Death & Disease. 2019; 10: 879.

[33] Li XJ, Ong CK, Cao Y, Xiang YQ, Shao JY, Ooi A, *et al*. Serglycin is a theranostic target in nasopharyngeal carcinoma that promotes metastasis. Cancer Research. 2011; 71: 3162–3172.

[34] Müller A, Homey B, Soto H, Ge N, Catron D, Buchanan ME, *et al*. Involvement of chemokine receptors in breast cancer metastasis. Nature. 2001; 410: 50–56.

[35] Luo F, Liao Y, Cao E, Yang Y, Tang K, Zhou D, *et al*. Hypermethylation of HIC2 is a potential prognostic biomarker and tumor suppressor of glioma based on bioinformatics analysis and experiments. CNS Neuroscience & Therapeutics. 2023; 29: 1154–1167.

[36] Chandrashekar DS, Bashel B, Balasubramanya SAH, Creighton CJ, Ponce-Rodriguez I, Chakravarthi BVSK, *et al*. UALCAN: A Portal for Facilitating Tumor Subgroup Gene Expression and Survival Analyses. Neoplasia (New York, N.Y.). 2017; 19: 649–658.

[37] Zhang Q, Liu W, Zhang HM, Xie GY, Miao YR, Xia M, *et al*. hTFtarget: A Comprehensive Database for Regulations of Human Transcription Factors and Their Targets. Genomics, Proteomics & Bioinformatics. 2020; 18: 120–128.

[38] Kolmykov S, Yevshin I, Kulyashov M, Sharipov R, Kondrakhin Y, Makeev VJ, *et al*. GTRD: an integrated view of transcription regulation. Nucleic Acids Research. 2021; 49: D104–D111.

[39] Zhang ZF, Huang TJ, Zhang XK, Xie YJ, Lin ST, Luo FF, *et al*. AKR1C2 acts as a targetable oncogene in esophageal squamous cell carcinoma via activating PI3K/AKT signaling pathway. Journal of Cellular and Molecular Medicine. 2020; 24: 9999–10012.

[40] Brabletz T, Kalluri R, Nieto MA, Weinberg RA. EMT in cancer. Nature Reviews. Cancer. 2018; 18: 128–134.

[41] Wang J, Yu L, Sun Y, Zhang L, Tu M, Cai L, *et al*. Development and Evaluation of Serum CST1 Detection for Early Diagnosis of Esophageal Squamous Cell Carcinoma. Cancer Management and Research. 2021; 13: 8341–8352.

[42] Vizeacoumar FS, Guo H, Dwernychuk L, Zaidi A, Freywald A, Wu FX, *et al*. Mining the plasma-proteome associated genes in patients with gastro-esophageal cancers for biomarker discovery. Scientific Reports. 2021; 11: 7590.

[43] Blanco MA, LeRoy G, Khan Z, Alečković M, Zee BM, Garcia BA, *et al*. Global secretome analysis identifies novel mediators of bone metastasis. Cell Research. 2012; 22: 1339–1355.

[44] Lin J, Liu W, Luan T, Yuan L, Jiang W, Cai H, *et al*. High expression of PU.1 is associated with Her-2 and shorter survival in patients with breast cancer. Oncology Letters. 2017; 14: 8220–8226.

[45] Song LJ, Zhang WJ, Chang ZW, Pan YF, Zong H, Fan QX, *et al*. PU.1 Is Identified as a Novel Metastasis Suppressor in Hepatocellular Carcinoma Regulating the miR-615-5p/IGF2 Axis. Asian Pacific Journal of Cancer Prevention: APJCP. 2015; 16: 3667–3671.

[46] Yao J, Duan L, Huang X, Liu J, Fan X, Xiao Z, *et al*. Development and Validation of a Prognostic Gene Signature Correlated with M2 Macrophage Infiltration in Esophageal Squamous Cell Carcinoma. Frontiers in Oncology. 2021; 11: 769727.

[47] Bahramian S, Sahebi R, Roohinejad Z, Delshad E, Javid N, Amini A, *et al*. Low expression of LncRNA-CAF attributed to the high expression of HIF1A in esophageal squamous cell carcinoma and gastric cancer patients. Molecular Biology Reports. 2022; 49: 895–905.

[48] Wang J, Wang X, Guo Y, Ye L, Li D, Hu A, *et al*. Therapeutic targeting of SPIB/SPI1-facilitated interplay of cancer cells and neutrophils inhibits aerobic glycolysis and cancer progression.

Clinical and Translational Medicine. 2021; 11: e588.

[49] Bhat AA, Nisar S, Maacha S, Carneiro-Lobo TC, Akhtar S, Siveen KS, *et al*. Cytokine-chemokine network driven metastasis in esophageal cancer; promising avenue for targeted therapy. Molecular Cancer. 2021; 20: 2.

[50] Kai F, Drain AP, Weaver VM. The Extracellular Matrix Modulates the Metastatic Journey. Developmental Cell. 2019; 49: 332–346.

[51] Lin EW, Karakasheva TA, Hicks PD, Bass AJ, Rustgi AK. The tumor microenvironment in esophageal cancer. Oncogene. 2016; 35: 5337–5349.

[52] Fang M, Yuan J, Peng C, Li Y. Collagen as a double-edged sword in tumor progression. Tumour Biology: the Journal of the International Society for Oncodevelopmental Biology and Medicine. 2014; 35: 2871–2882.

[53] Northcott JM, Dean IS, Mouw JK, Weaver VM. Feeling Stress: The Mechanics of Cancer Progression and Aggression. Frontiers in Cell and Developmental Biology. 2018; 6: 17.

[54] Lei Z, Jian M, Li X, Wei J, Meng X, Wang Z. Biosensors and bioassays for determination of matrix metalloproteinases: state of the art and recent advances. Journal of Materials Chemistry. B. 2020; 8: 3261–3291.

[55] Lu H, Bhat AA, Peng D, Chen Z, Zhu S, Hong J, *et al*. APE1 Upregulates MMP-14 via Redox-Sensitive ARF6-Mediated Recycling to Promote Cell Invasion of Esophageal Adenocarcinoma. Cancer Research. 2019; 79: 4426–4438.

[56] Dinh HQ, Pan F, Wang G, Huang QF, Olingy CE, Wu ZY, *et al*. Integrated single-cell transcriptome analysis reveals heterogeneity of esophageal squamous cell carcinoma microenvironment. Nature Communications. 2021; 12: 7335.